The atmospheric circulation of the EBUSs: the coastal inversion, winds, and weather systems

CLIVAR-ICTP Summer school
ICTP Trieste
15 July 2019

Thomas Toniazzo, NORCE Research, Bjerknes Centre, Bergen, Norway

Outline:

I. Coastal inversion and the coastal jet

II. Tropospheric temperatures and the inversion

III. Weather systems

IV. Observations and models

I. The coastal inversion and the coastal jet

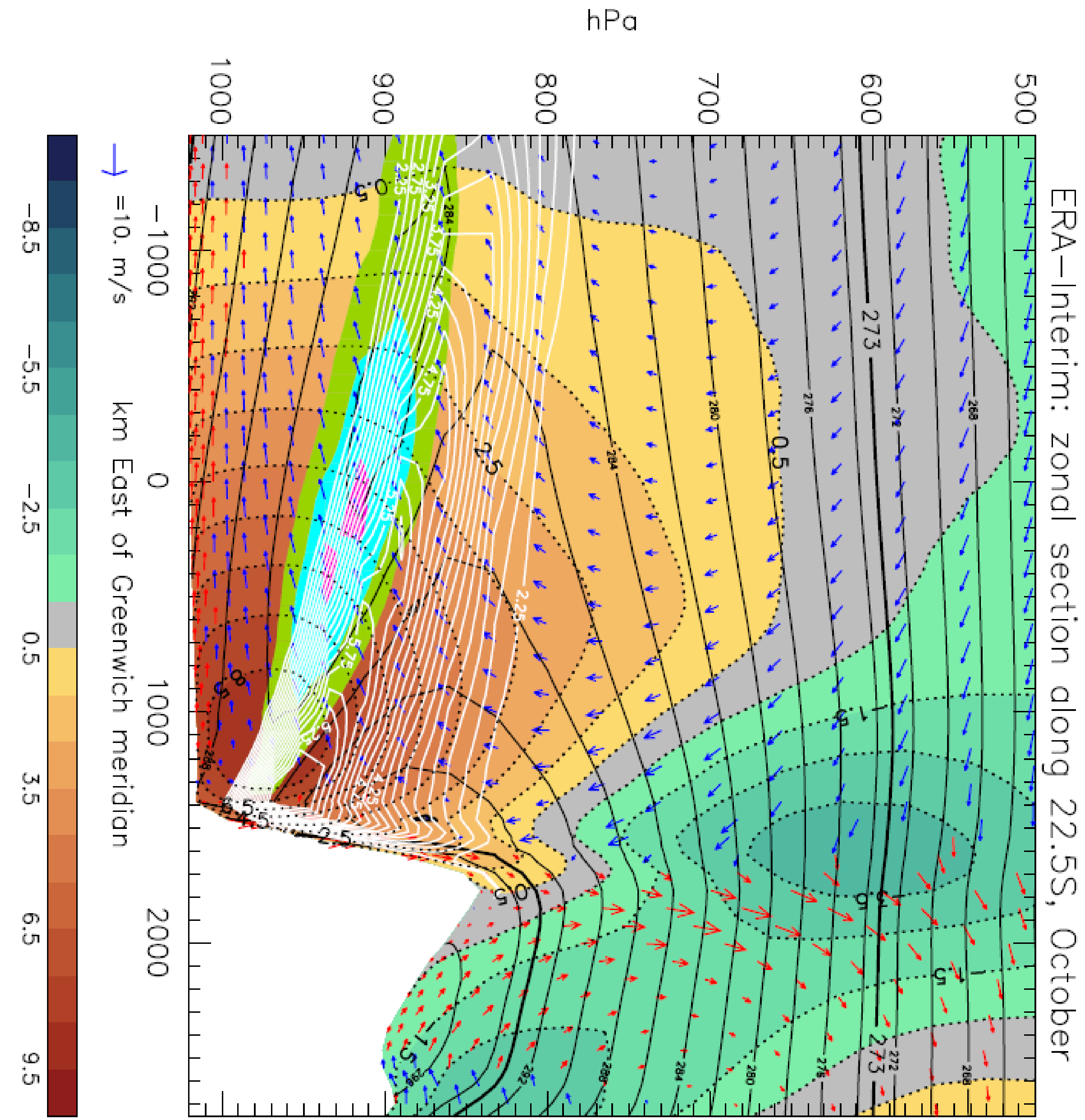

Figure 5: Zonal section along 22-23S in the Eastern Atlantic, illustrating the distribution of meridional (colour-filled, black dashed countours, spacing 0.5 m/s), zonal and vertical wind components (arrows, in red for ascent and in blue for descent; scale on the bottom left, in m/s for the zonal component, and mPa/s for the vertical component), temperature (black solid contour lines, spacing 2 K, plus 0 ^{0}C and 20 ^{0}C isotherms as thicker black lines), static stability (white contour lines, spacing $0.5\times10^{-2}s^{-1}$ between $2.25\times10^{-2}s^{-1}$ and $4.25\times10^{-2}s^{-1}$, and cloud concentration (above 0.2, 0.3 and 0.4, colour-filled in green, cyan, and magenta, respectively). October climatology from ERA-Interim data.

Thermal wind balance of the meridional jet

Geostrophic balance: $$f\,v = \partial_x \Phi$$

Hydrostatic balance: $$f\,\partial_p v = -\frac{R}{p}\left(\partial_x T\right)_p$$

$$= -\frac{1}{\rho}\left(\partial_x \ln\theta\right)_p$$

Assume: $$\partial_x \theta \approx \partial_p \theta\, \partial_x p_i$$

where $\boldsymbol{p_i}$ is the level of the inversion; then

$$\partial_p v \approx -\frac{N_i^2}{f\,g^2 \rho_i^2}\left(\partial_x p_i\right)_p$$

or also

$$\partial_z v \approx \frac{N_i^2}{f\,g\,\rho_i}\left(\partial_x p_i\right)_p$$

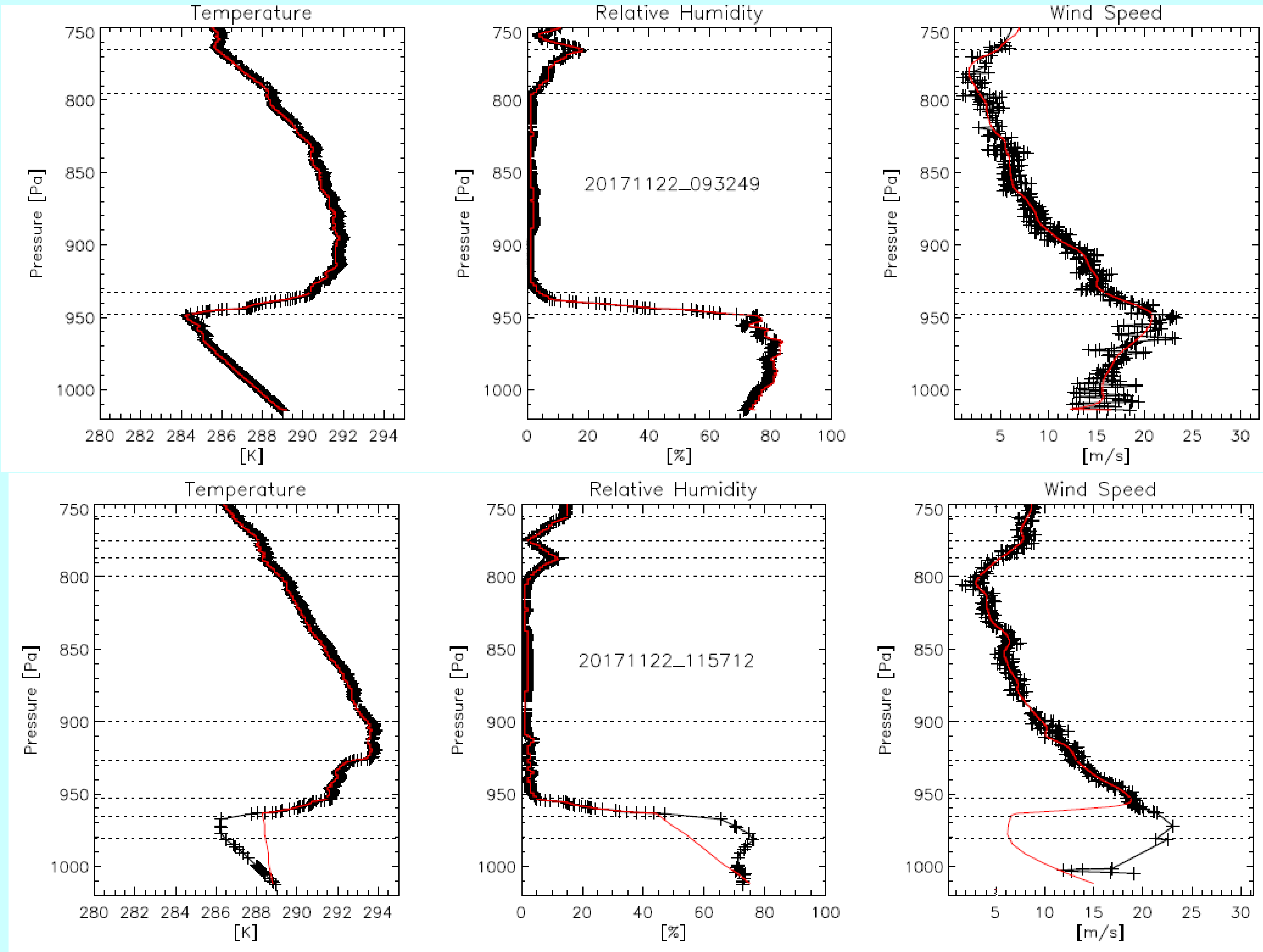
Temperature
Pressure [Pa]
[K]
Relative Humidity
20171122_093249
[%]
Wind Speed
[m/s]
Temperature
Pressure [Pa]
[K]
Relative Humidity
20171122_115712
[%]
Wind Speed
[m/s]

Inversion slope ~18hPa/39km

Using:

$$\partial_z v \approx \frac{N_i^{\,2}}{f g \rho_i} \left(\partial_x p_i \right)_p$$

$$\Delta v \approx \frac{(\Delta \theta)_i}{f \theta \rho_i} \frac{\Delta p_i}{\Delta x} \approx 15\, m/s$$

Back to the trade winds and the Benguela jet

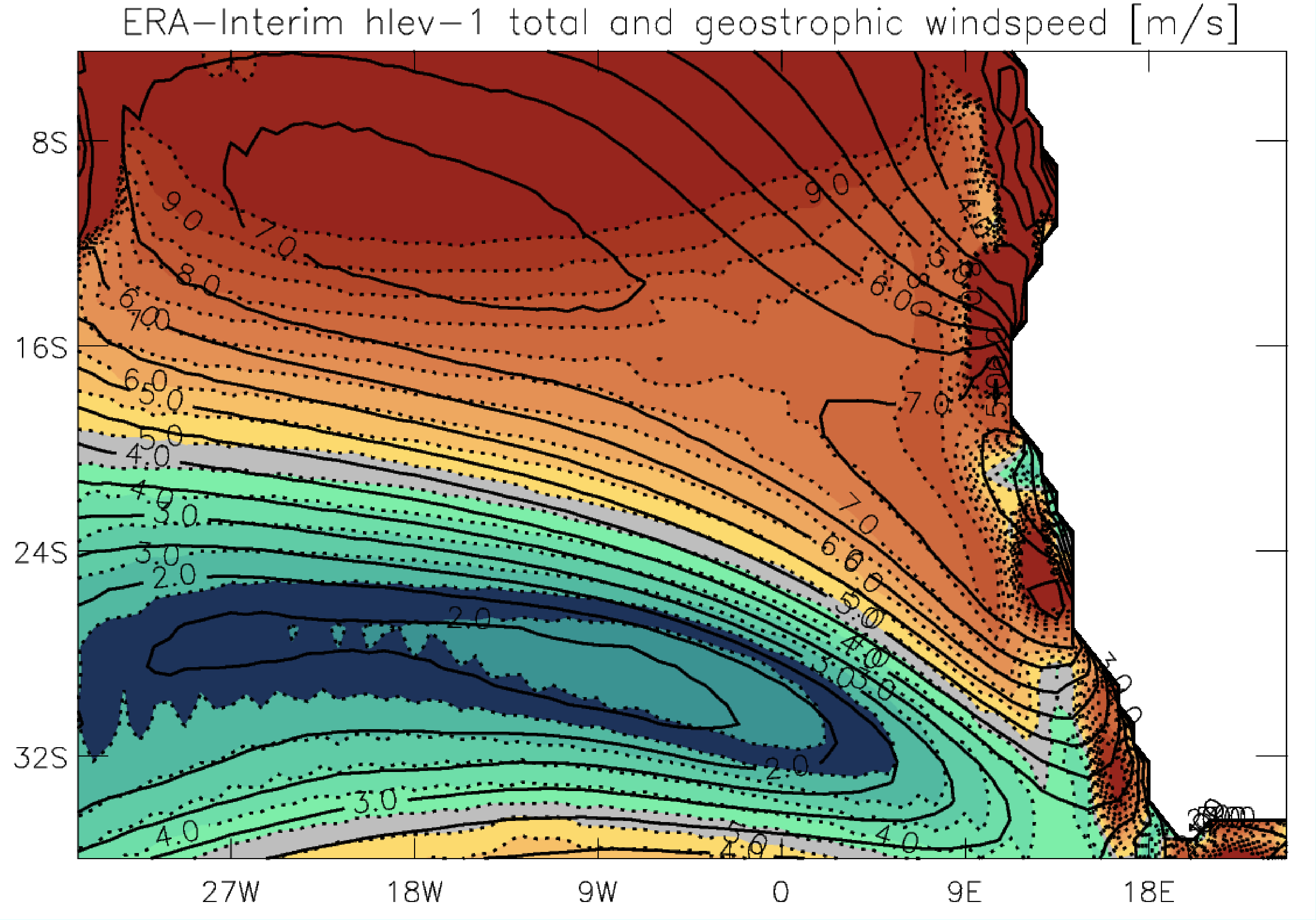

Back to the trade winds and the Benguela jet

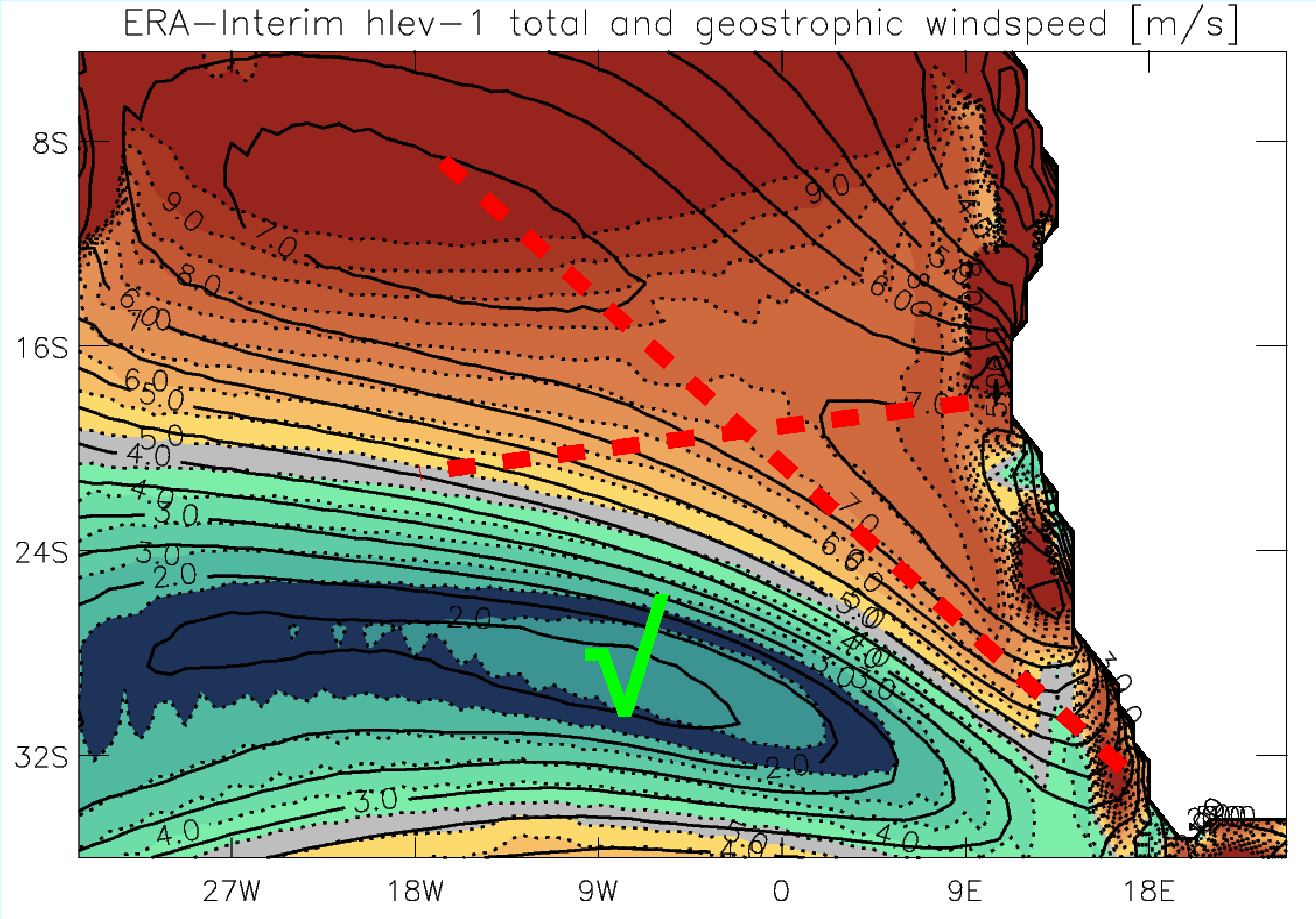

Back to the trade winds and the Benguela jet

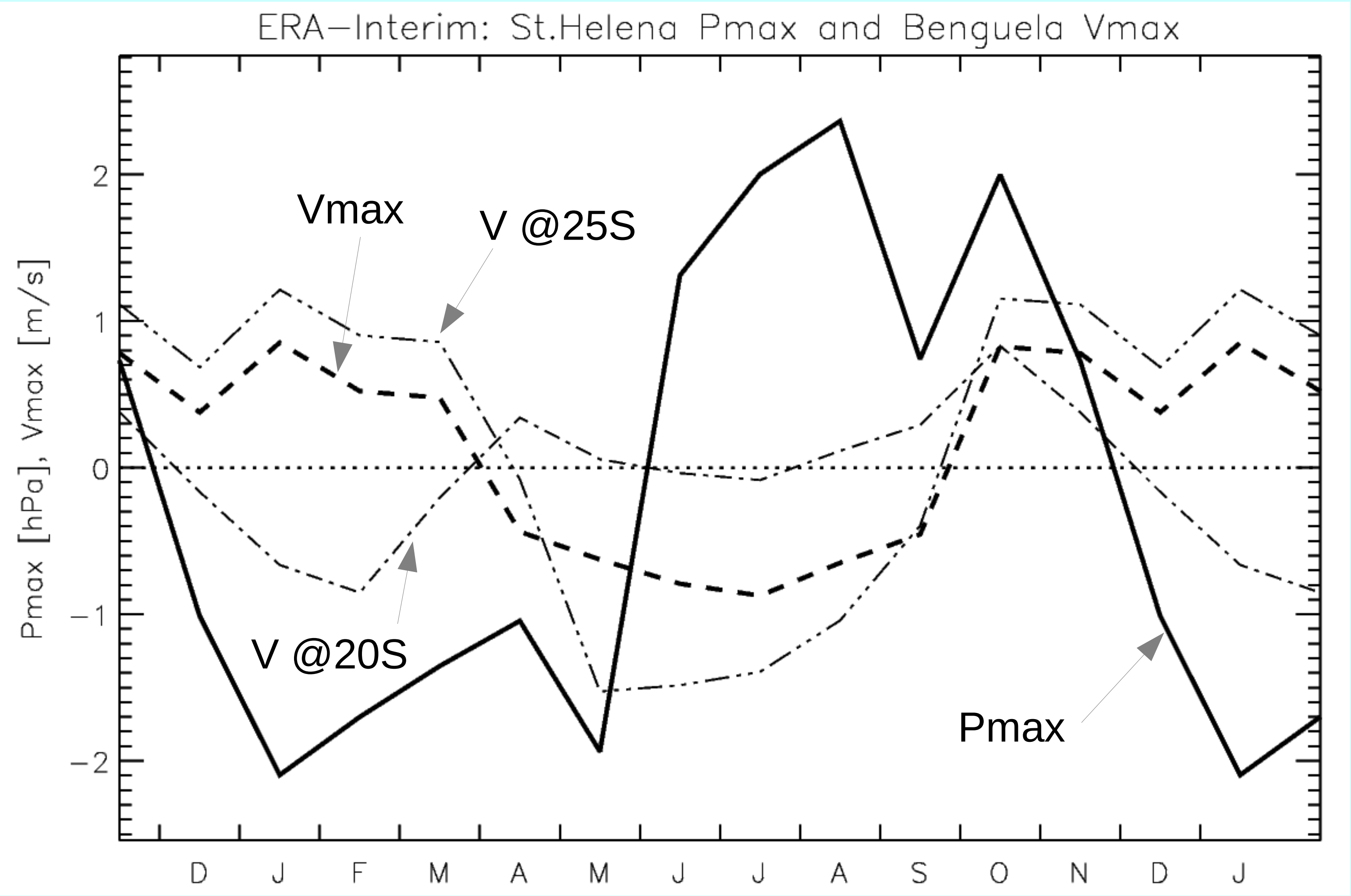

Back to the trade winds and the Benguela jet

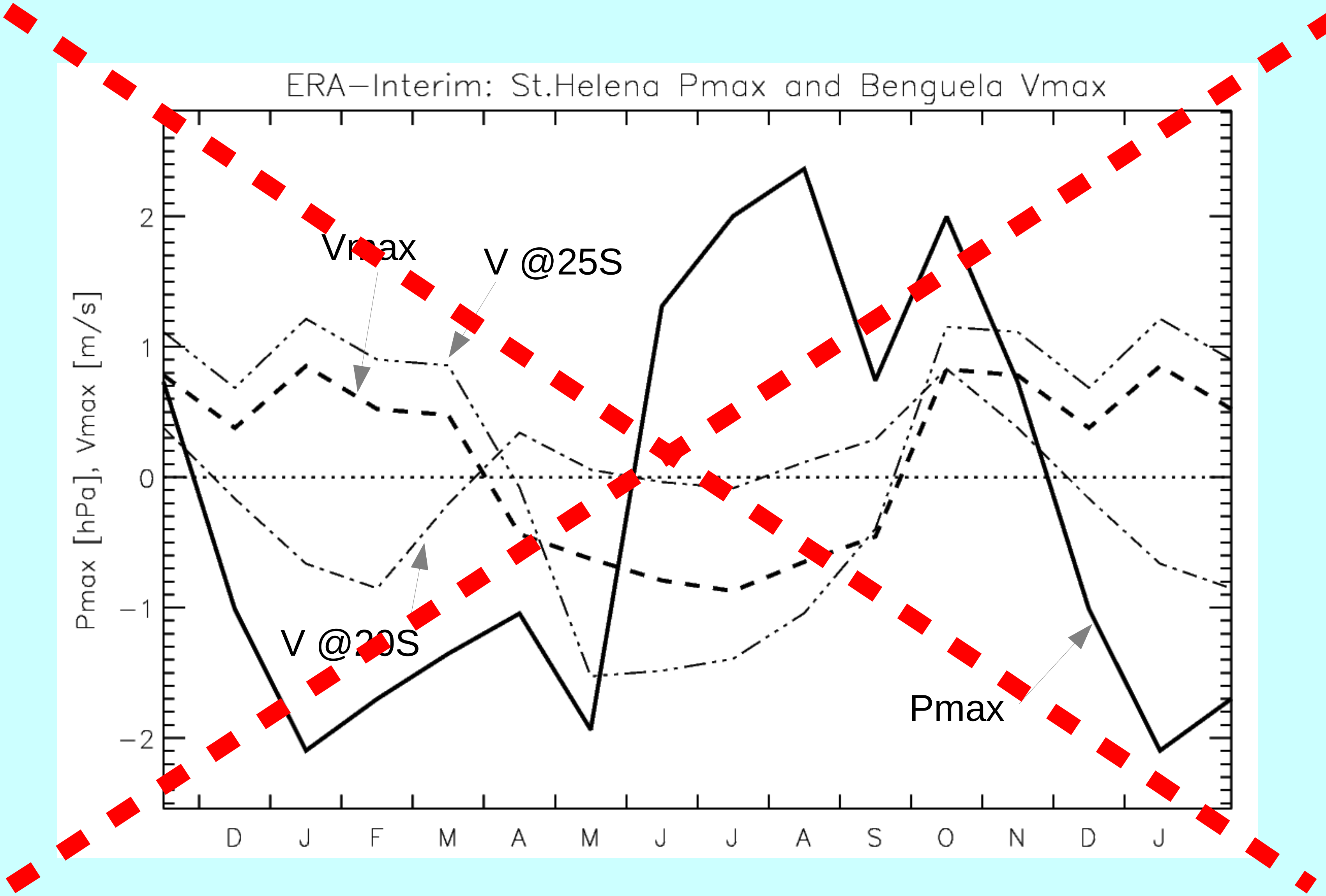

Munoz & Garreaud (2005): momentum budget of the Chilean coastal LLJ

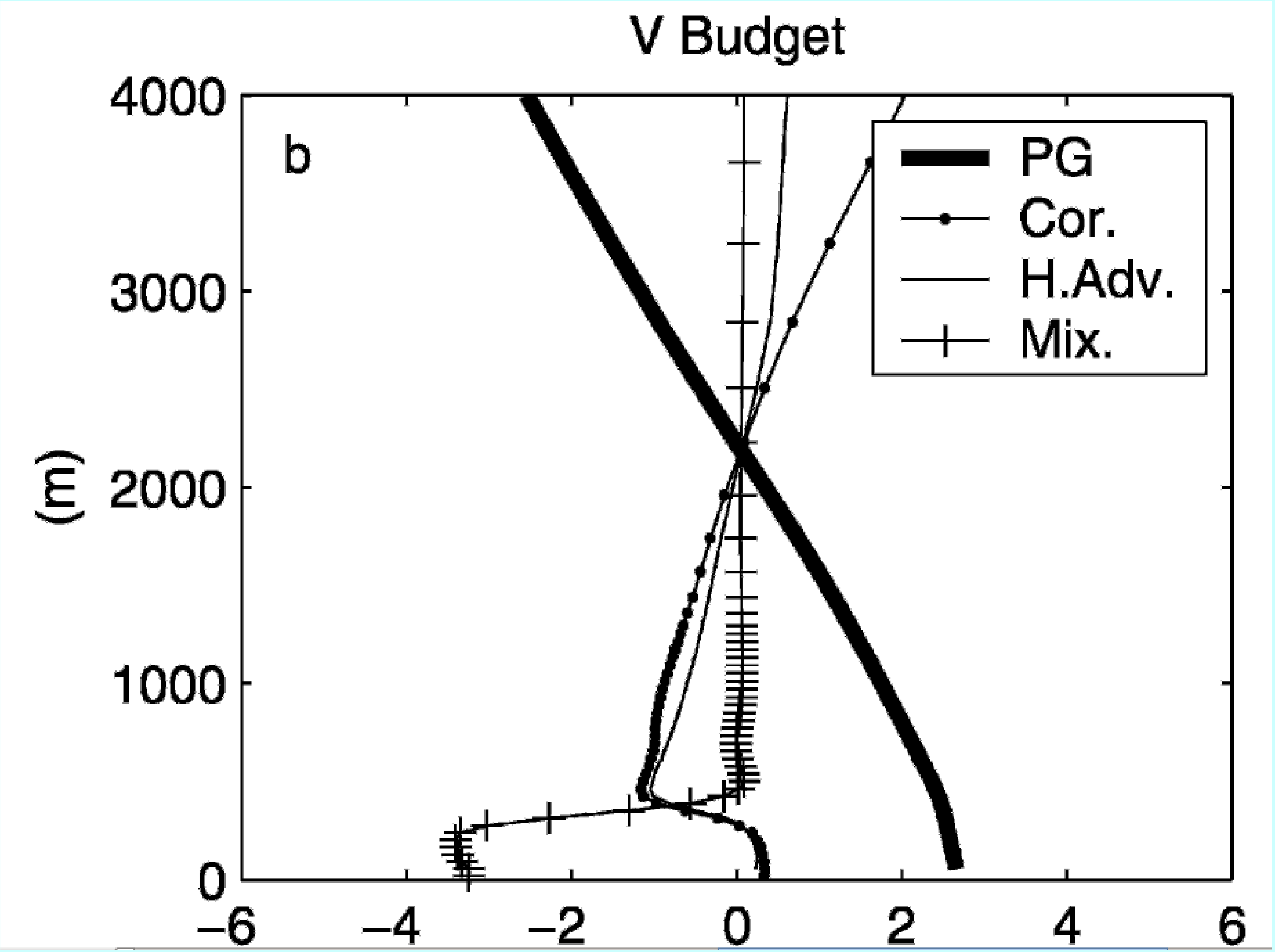

The BLLJ

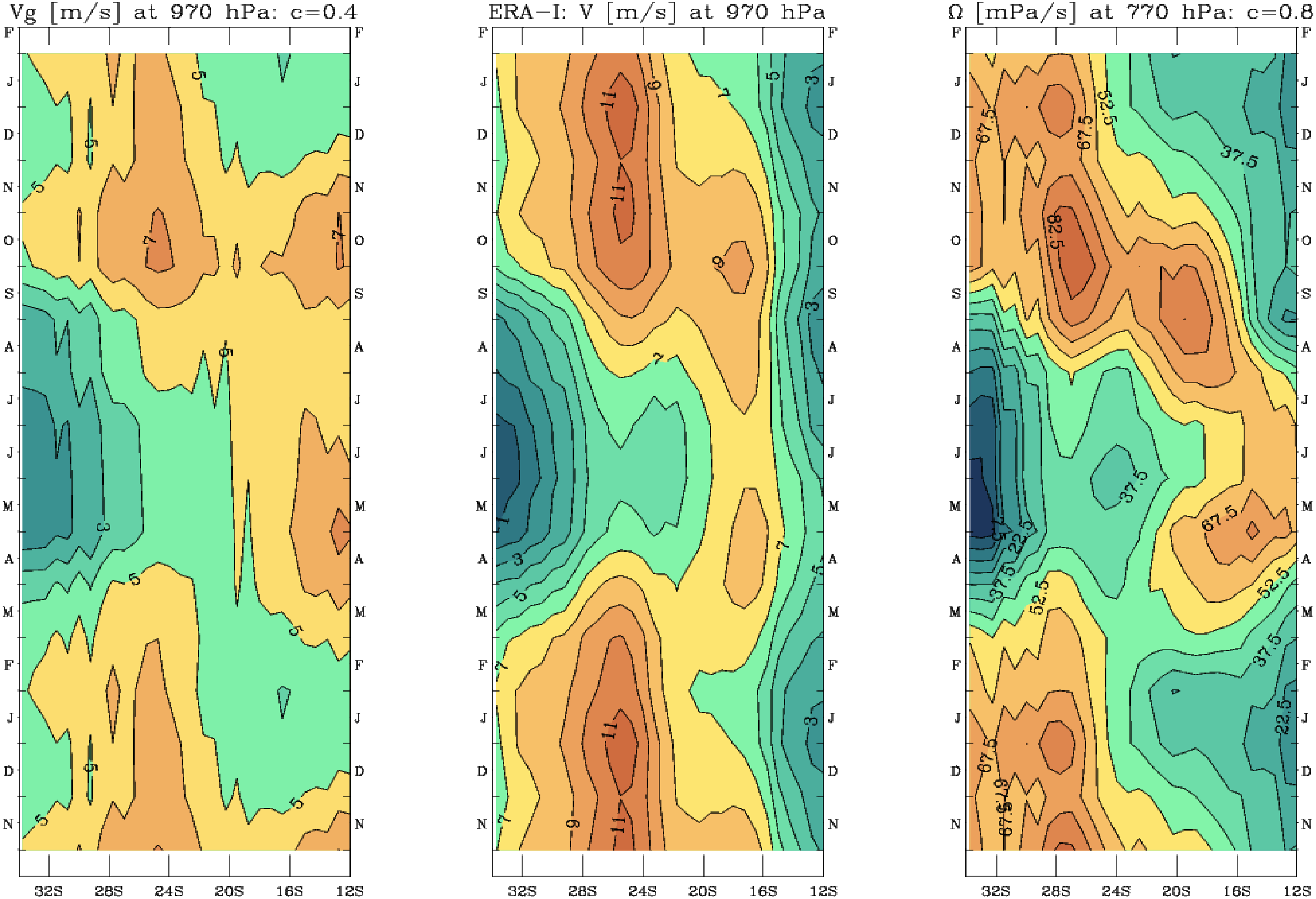

Vg [m/s] at 970 hPa: c=0.4
ERA-I: V [m/s] at 970 hPa
Ω [mPa/s] at 770 hPa: c=0.8
F
J
D
N
O
S
A
J
J
M
A
M
F
J
D
N
32S
28S
24S
20S
16S
12S

The BLLJ is primarily controlled by subsidence

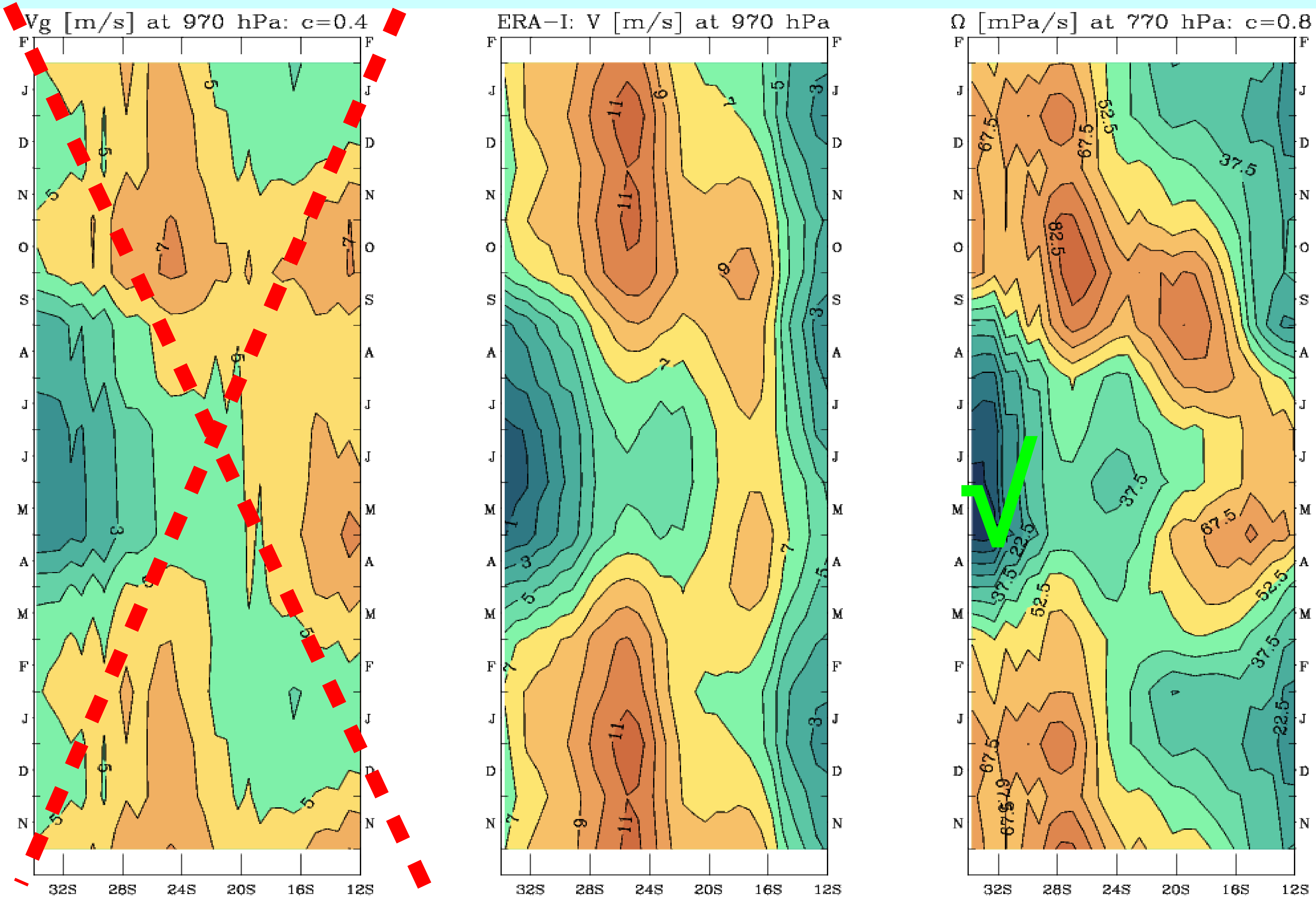

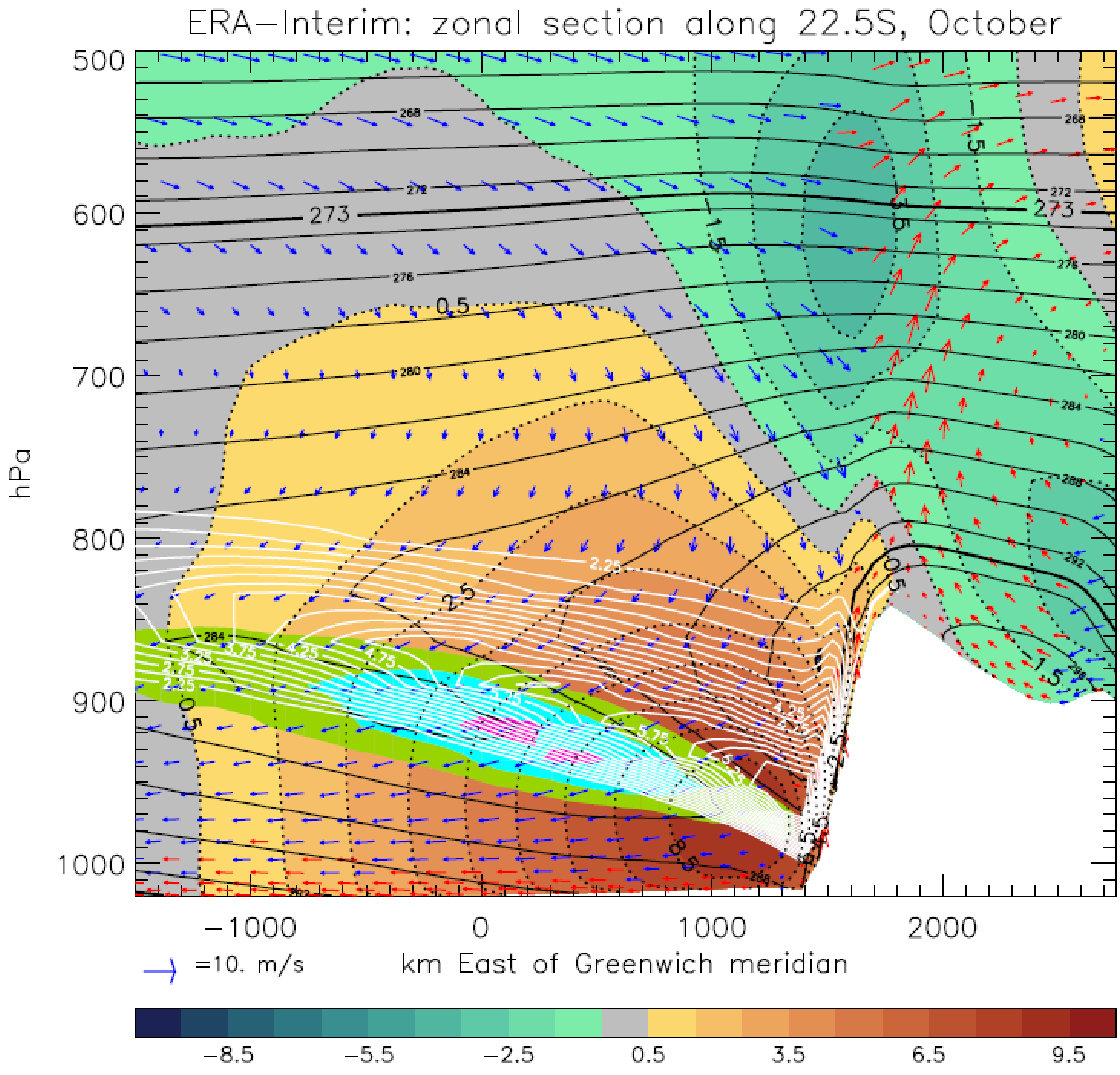

Figure 5: Zonal section along 22-23S in the Eastern Atlantic, illustrating the distribution of meridional (colour-filled, black dashed contours, spacing 0.5 m/s), zonal and vertical wind components (arrows, in red for ascent and in blue for descent; scale on the bottom left, in m/s for the zonal component, and mPa/s for the vertical component), temperature (black solid contour lines, spacing 2 K, plus 0 ^{0}C and 20 ^{0}C isotherms as thicker black lines), static stability (white contour lines, spacing $0.5\times10^{-2}s^{-1}$ between $2.25\times10^{-2}s^{-1}$ and $4.25\times10^{-2}s^{-1}$, and cloud concentration (above 0.2, 0.3 and 0.4, colour-filled in green, cyan, and magenta, respectively). October climatology from ERA-Interim data.

II. Tropospheric temperatures and the inversion

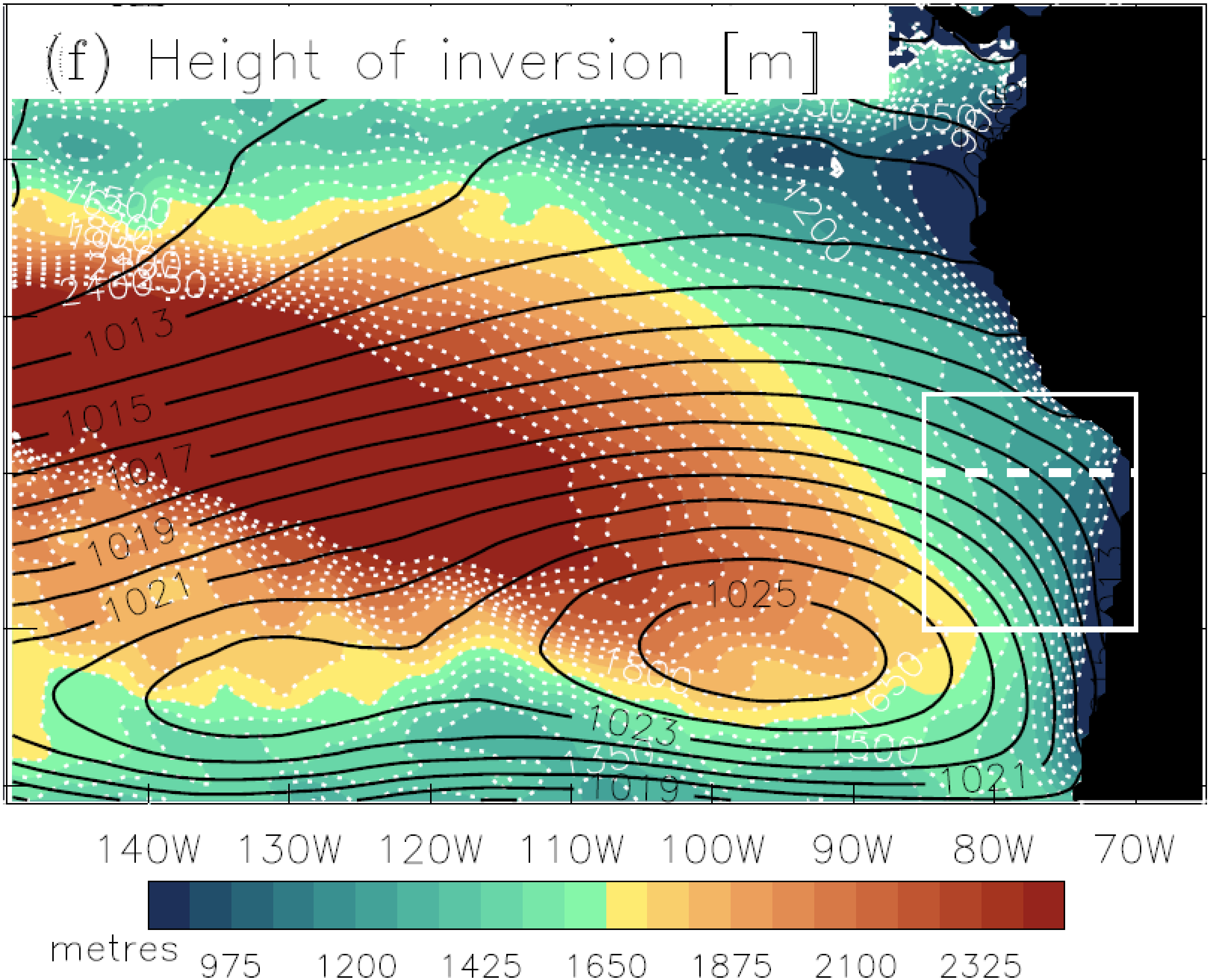
(f) Height of inversion [m]
1013
1015
1017
1019
1021
1023
1025
1019
1021
1200
1800
1650
1500
140W
130W
120W
110W
100W
90W
80W
70W
metres
975
1200
1425
1650
1875
2100
2325

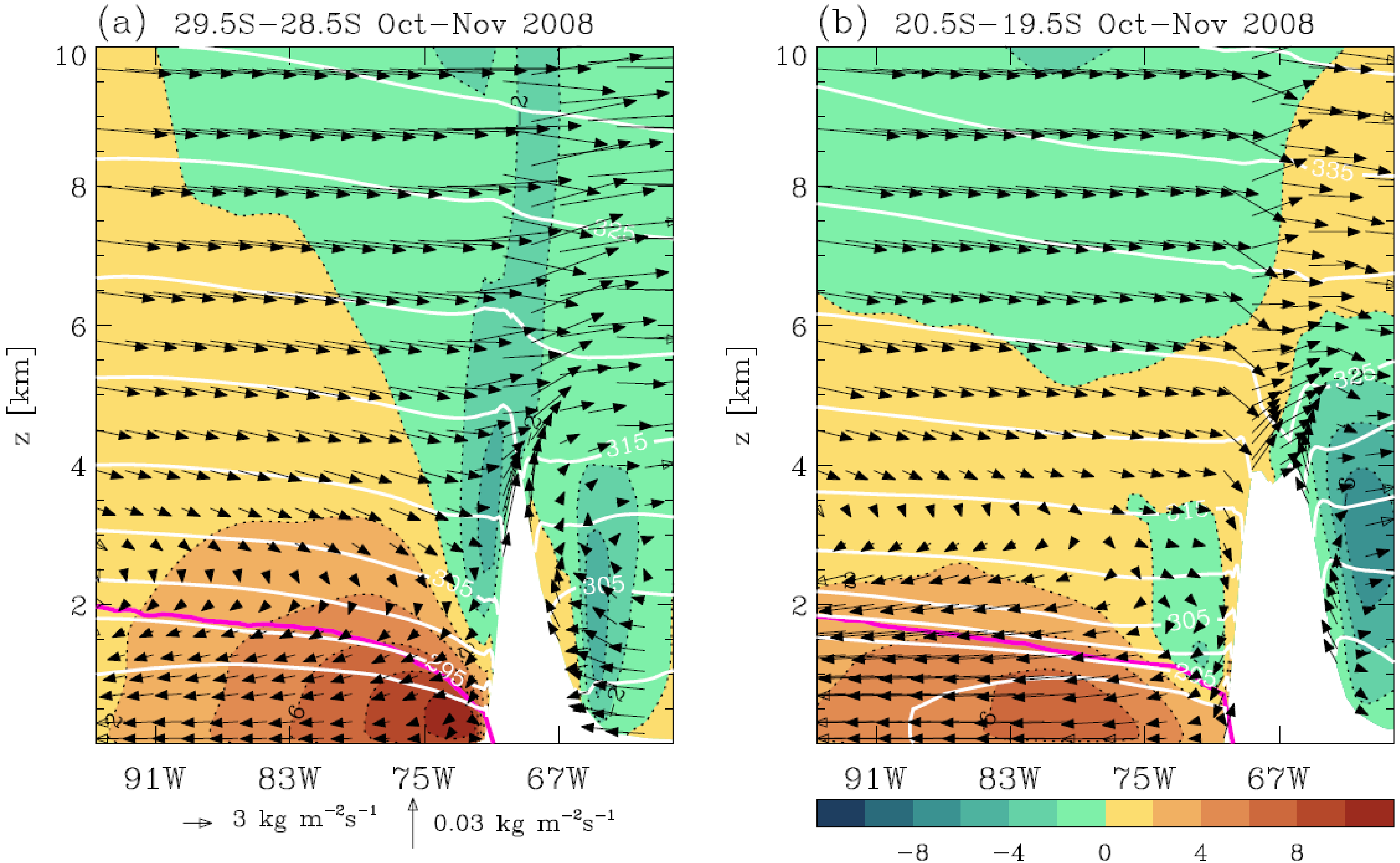

(a) 29.5S–28.5S Oct–Nov 2008
(b) 20.5S–19.5S Oct–Nov 2008
z [km]
10
8
6
4
2
91W
83W
75W
67W
325
315
305
295
335
3 kg m^{-2}s^{-1}
0.03 kg m^{-2}s^{-1}
−8
−4
0
4
8

Characteristics of the PBL inversion

(Toniazzo et al, 2011; & other VOCALs-REx work)

A typical vertical temperature profile in the STAC

- The PBL is nearly dry-adiabatic
- The cloud layer is moist-adiabatic
- The FT is superadiabatic, due to radiative cooling
- A miracle happens when plotting θ_w

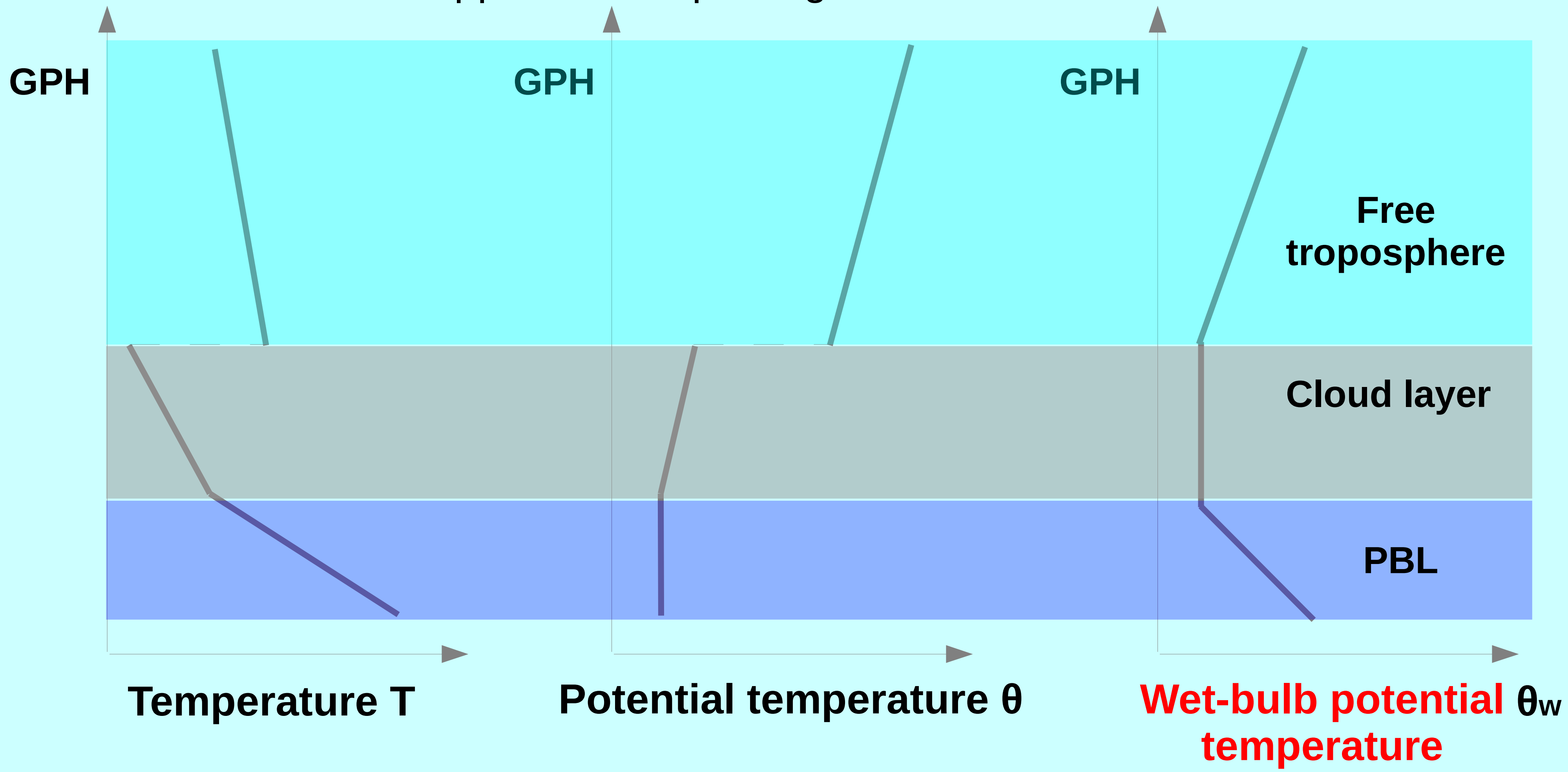

Characteristics of the PBL inversion

(Toniazzo et al, 2011; & other VOCALs-REx work)

- **θ_w** is conserved under adiabatic mixing.
- **$\Delta\theta_w \leq 0$** => (marginal) instability for mixing of FT and cloudy air.
- This allows energy-efficient entrainment in balance with FT subsidence.
- $\Delta\theta_w > 0$ (absolute stability) => reduced entrainment, inversion sinks
- $\Delta\theta_w << 0$ => PBL deepening
- In-situ data show a tendency for **$\Delta\theta_w \approx 0$** to be maintained for time-scales longer than 1-2 days

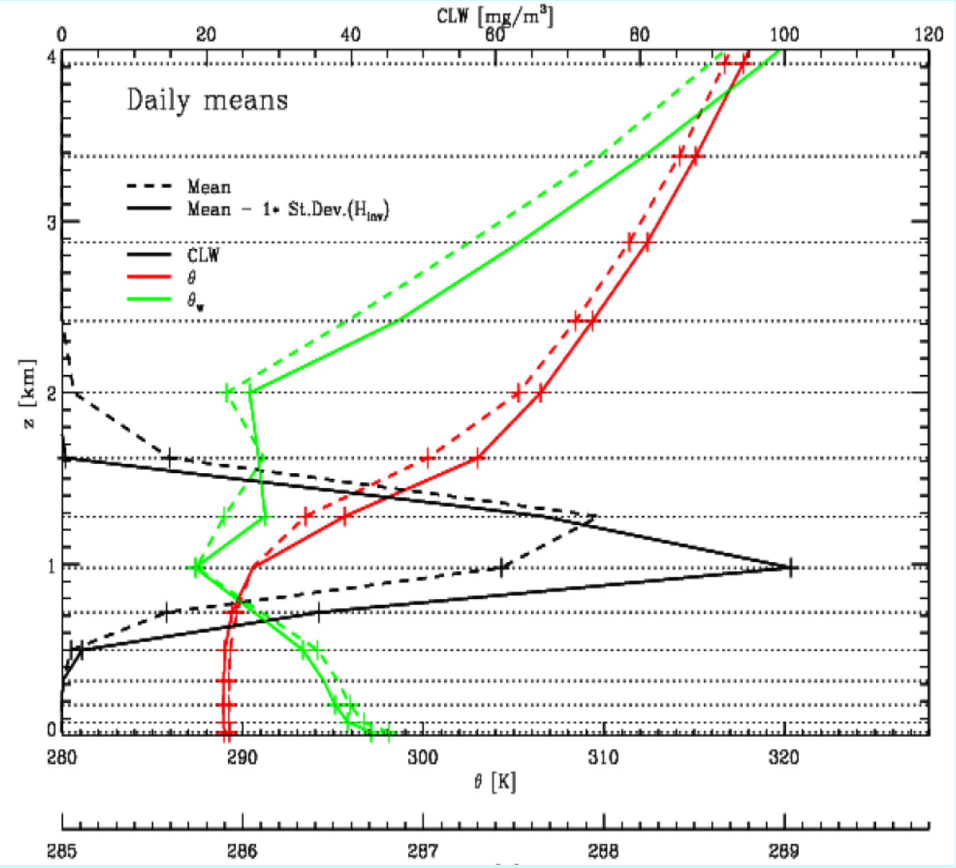

An interesting corollary: mixing-length scaling of entrainment process

$$\frac{\rho c_p}{\theta}\left(\partial_t + \underline{u}\cdot\underline{\nabla}\right)\theta = \frac{1}{T}\left[R - \dot{\rho}_e\left(c_p T\frac{\Delta\theta}{\theta} + L_c q_l\right)\right]$$

$$-\dot{m}_i \partial_z \theta_i \quad \frac{c_p}{\theta}$$

(radiative cooling)

$$-\rho\partial_z\left(\kappa\partial_z\theta_L\right)$$

$$\Delta z \sim \sqrt{\kappa}.$$

(Deardorff 1975)

Scaling from mixing-length (diffusive) approximation

$$\Delta z \sim \quad \lambda_e := \dot{m}_i/\dot{\rho}_e \quad \sim \quad \dot{m}_i/\rho$$

$$\lambda_e \mathrm{Ex}(p)\frac{\partial\theta}{\partial z} \simeq \mathrm{Ex}(p)\Delta\theta + \frac{L_c}{c_p}q_l$$

Characteristics of the PBL inversion

(Toniazzo et al, 2011; & other VOCALs-REx work)

→ a warming of the FT causes the inversion to sink and to strengthen

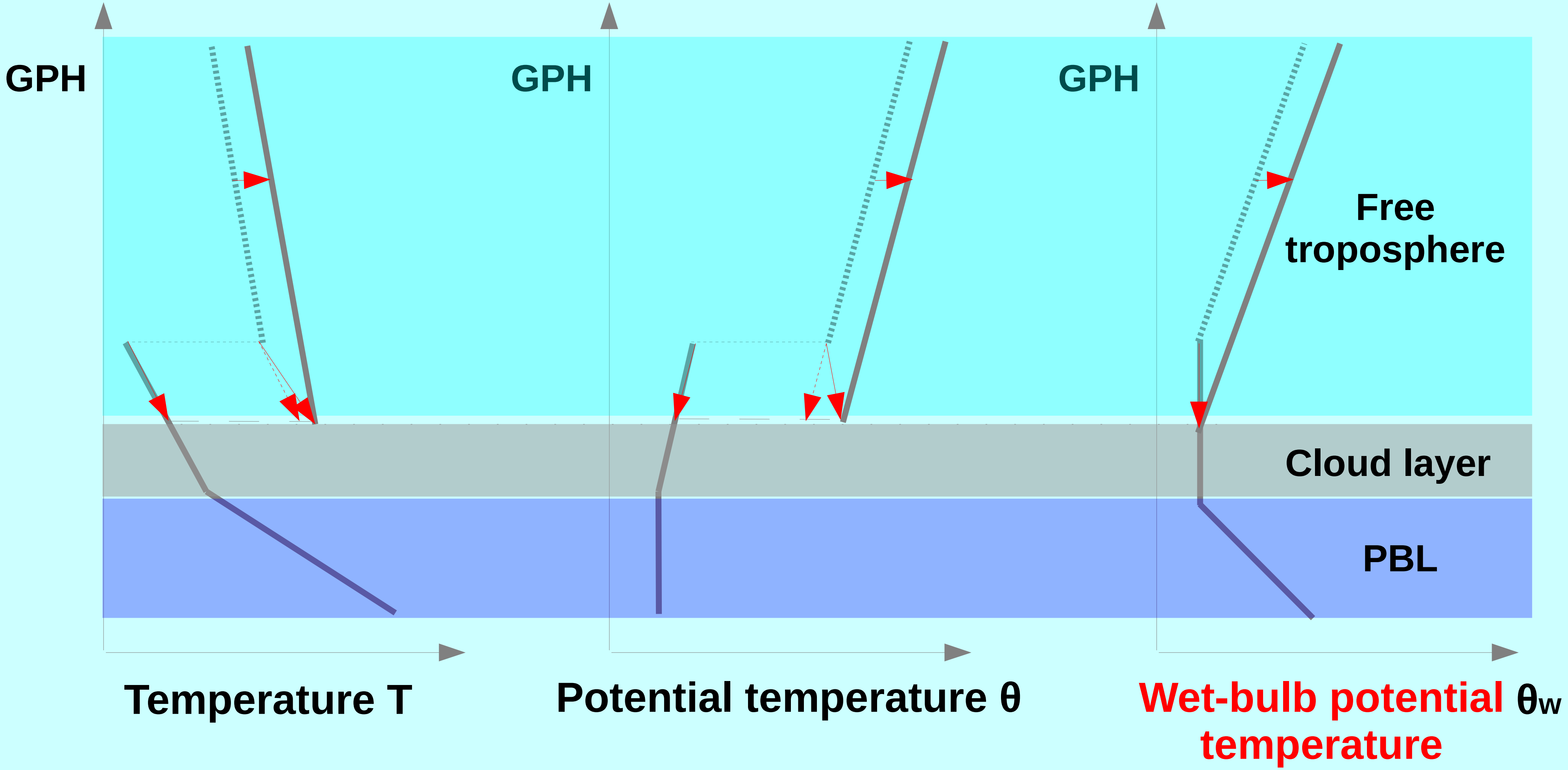

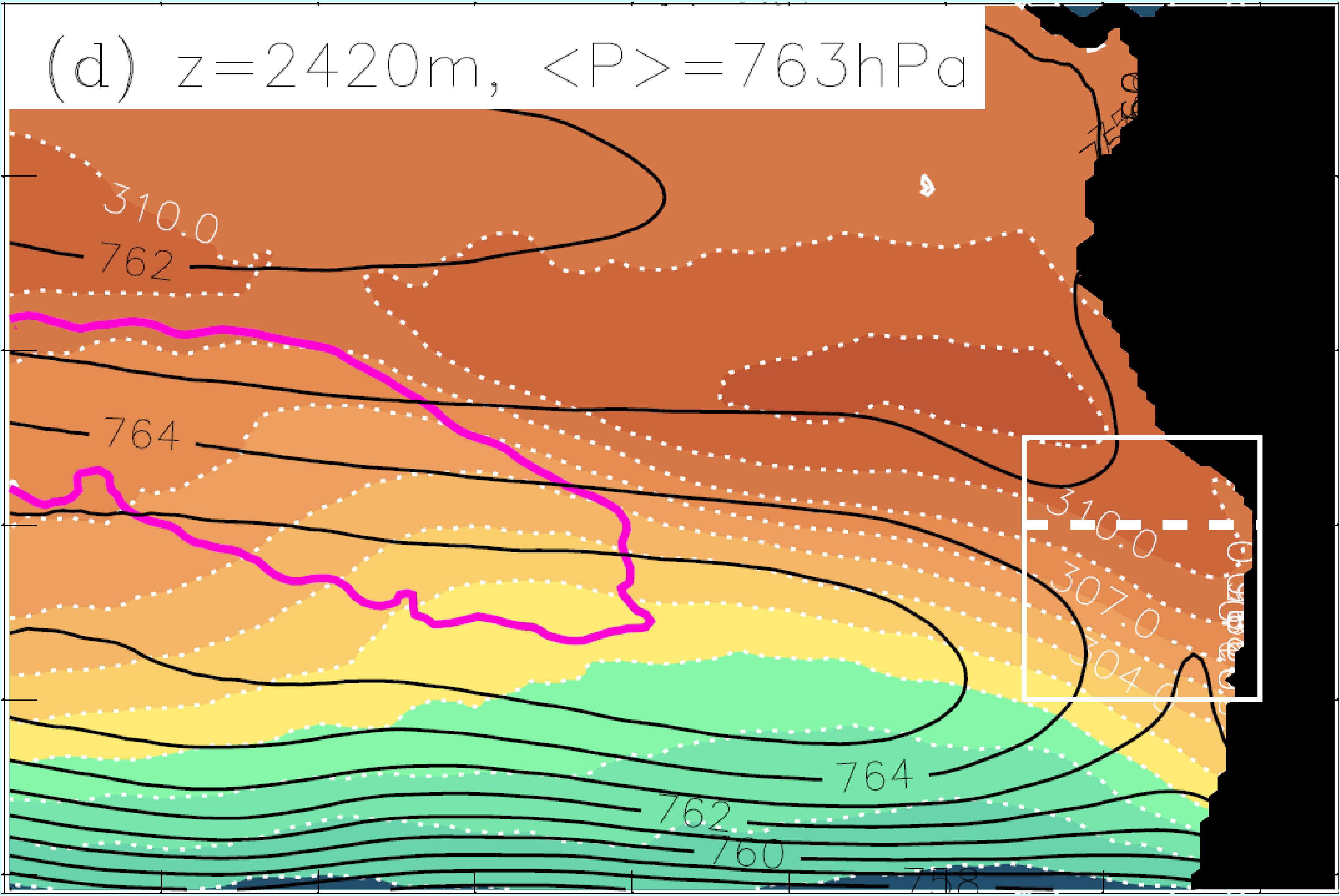
(d) z=2420m, <P>=763hPa
310.0
762
764
310.0
307.0
304.0
764
762
760

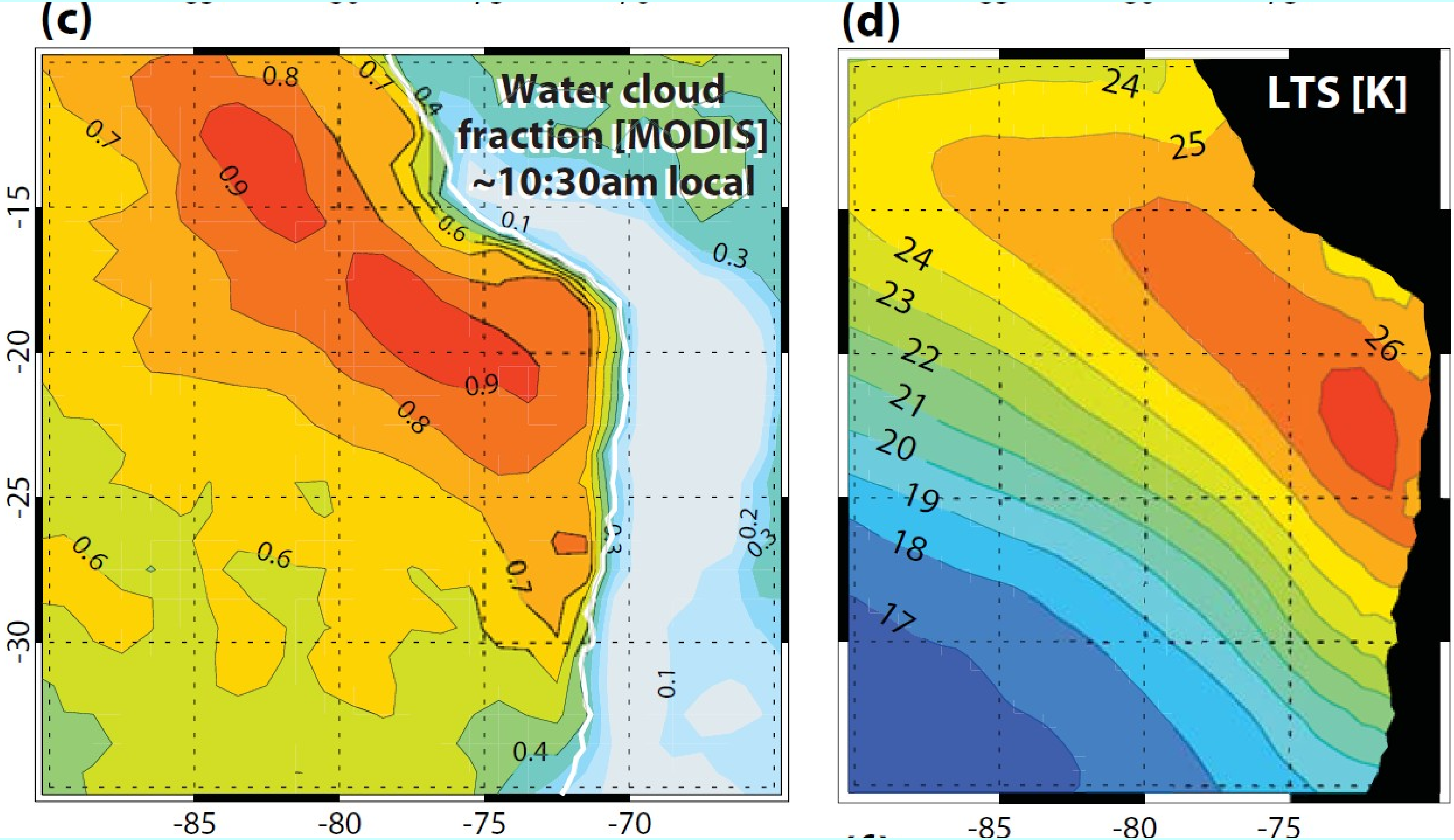
(c)
Water cloud
fraction [MODIS]
~10:30am local
0.8
0.7
0.7
0.9
0.6
0.1
0.3
0.9
0.8
0.6
0.6
0.7
0.3
0.2
0.3
0.1
0.4
-15
-20
-25
-30
-85
-80
-75
-70
(d)
LTS [K]
24
25
24
23
22
21
20
19
18
17
26
-85
-80
-75

1. **FT cooling favour high, weak inversion and low cloud cover.**
2. **Driven by cold, esp. vertical advection**
3. **FT warming has the opposite effect**
4. **Strong mid-latitude influences.**

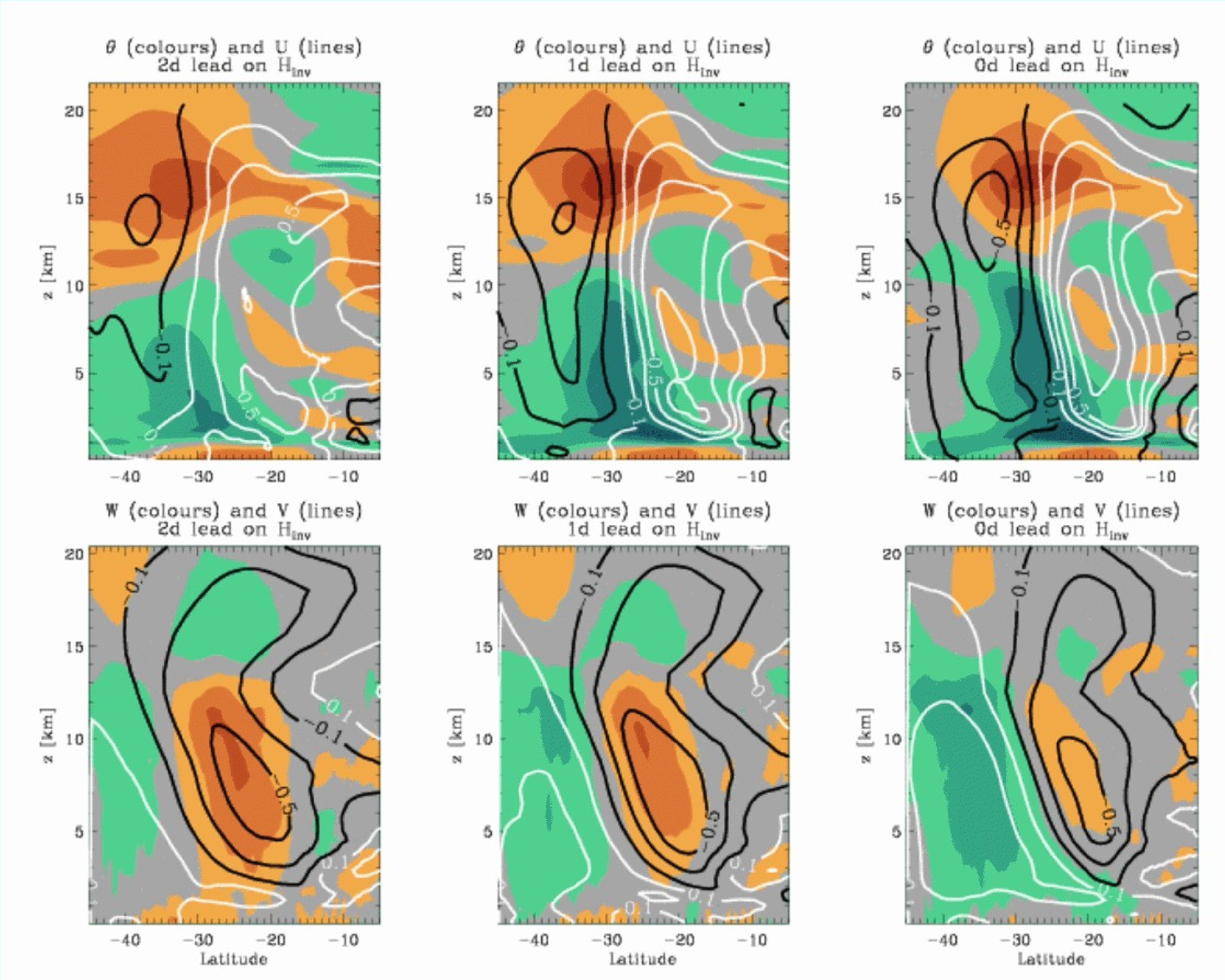

Interim 2:

1. FT cold advection favour high, weak inversion and low cloud cover.

2. FT warming has the opposite effect

3. Strong mid-latitude influences

4. Advection often dominated by vertical motion.

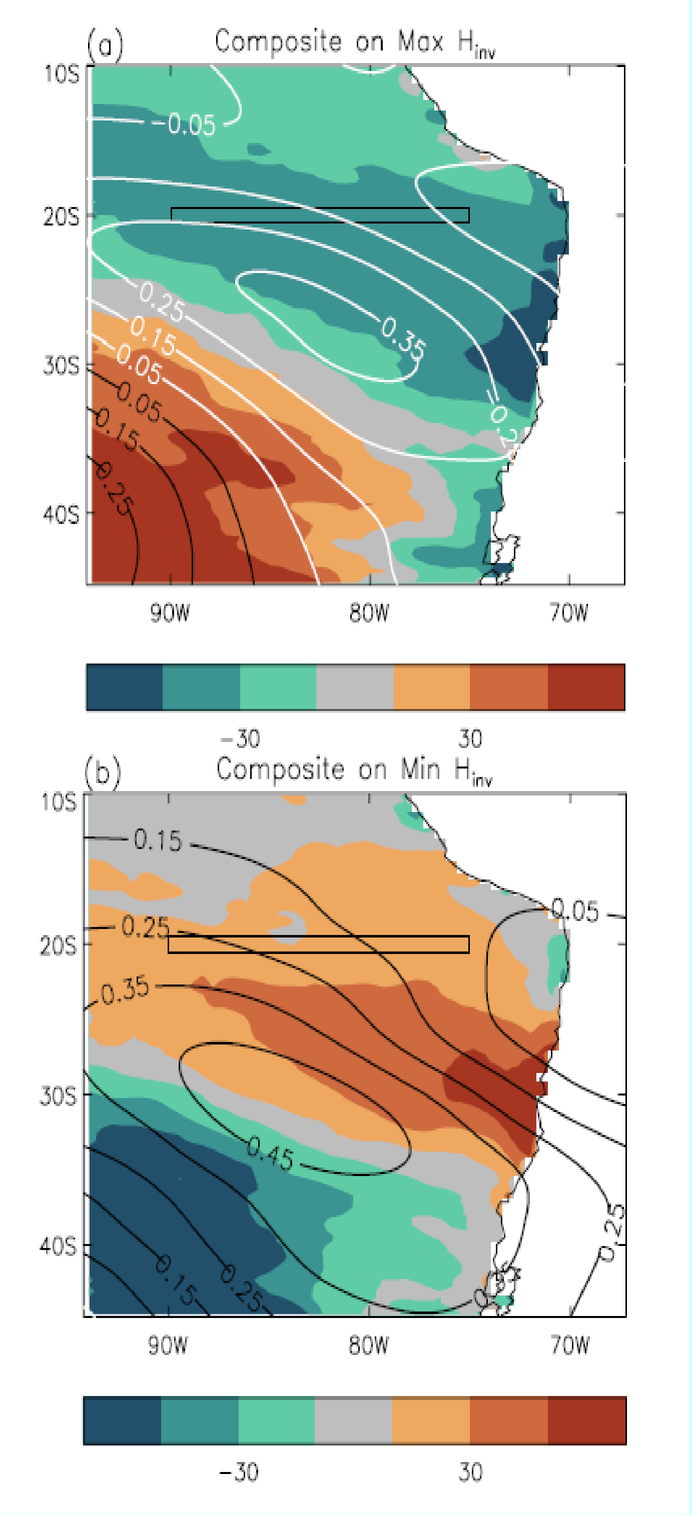

Interim 3:

1. **Subsidence and inversion strength are strongly related through dynamical-physical processes**

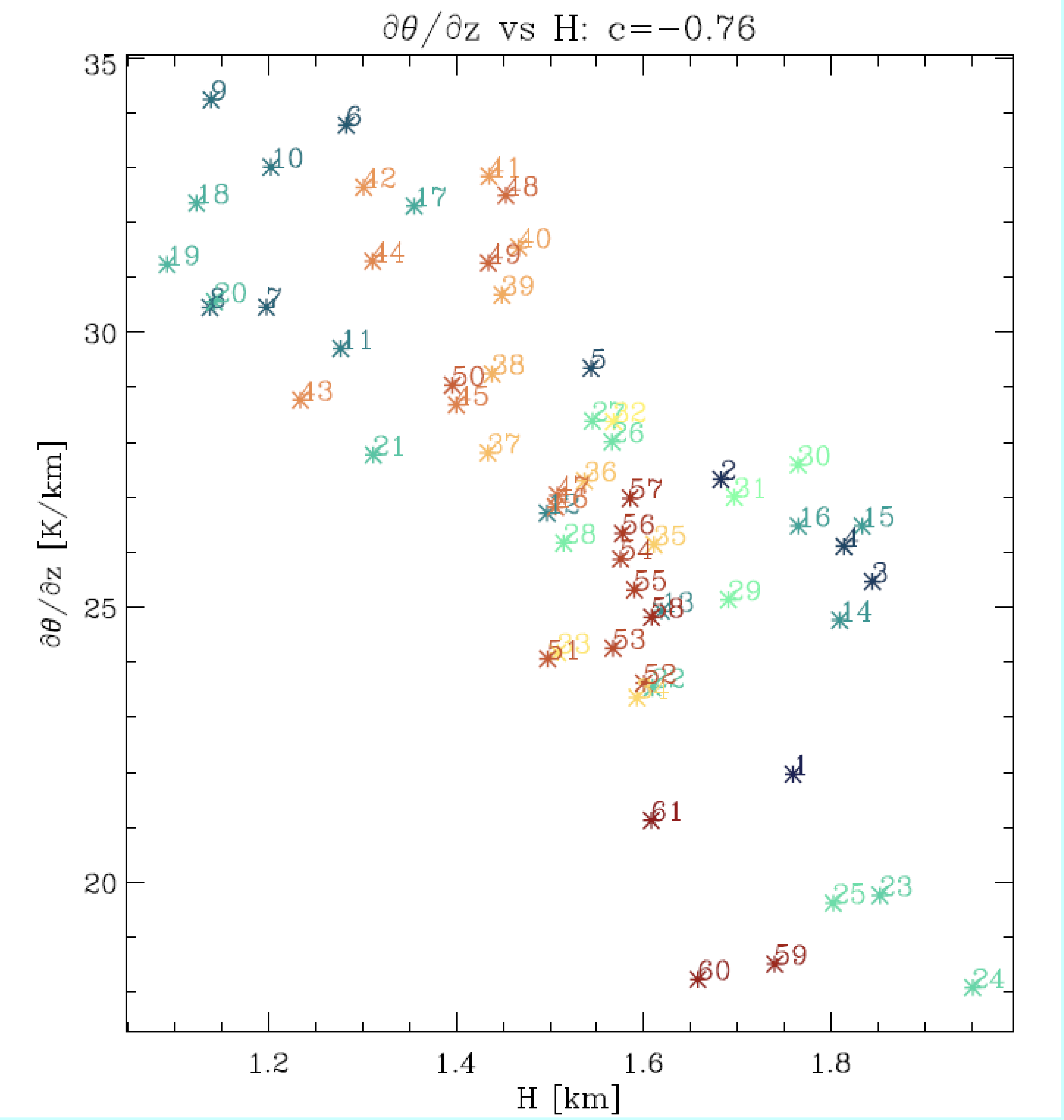

Importance of the **diurnal cycle** at low latitudes

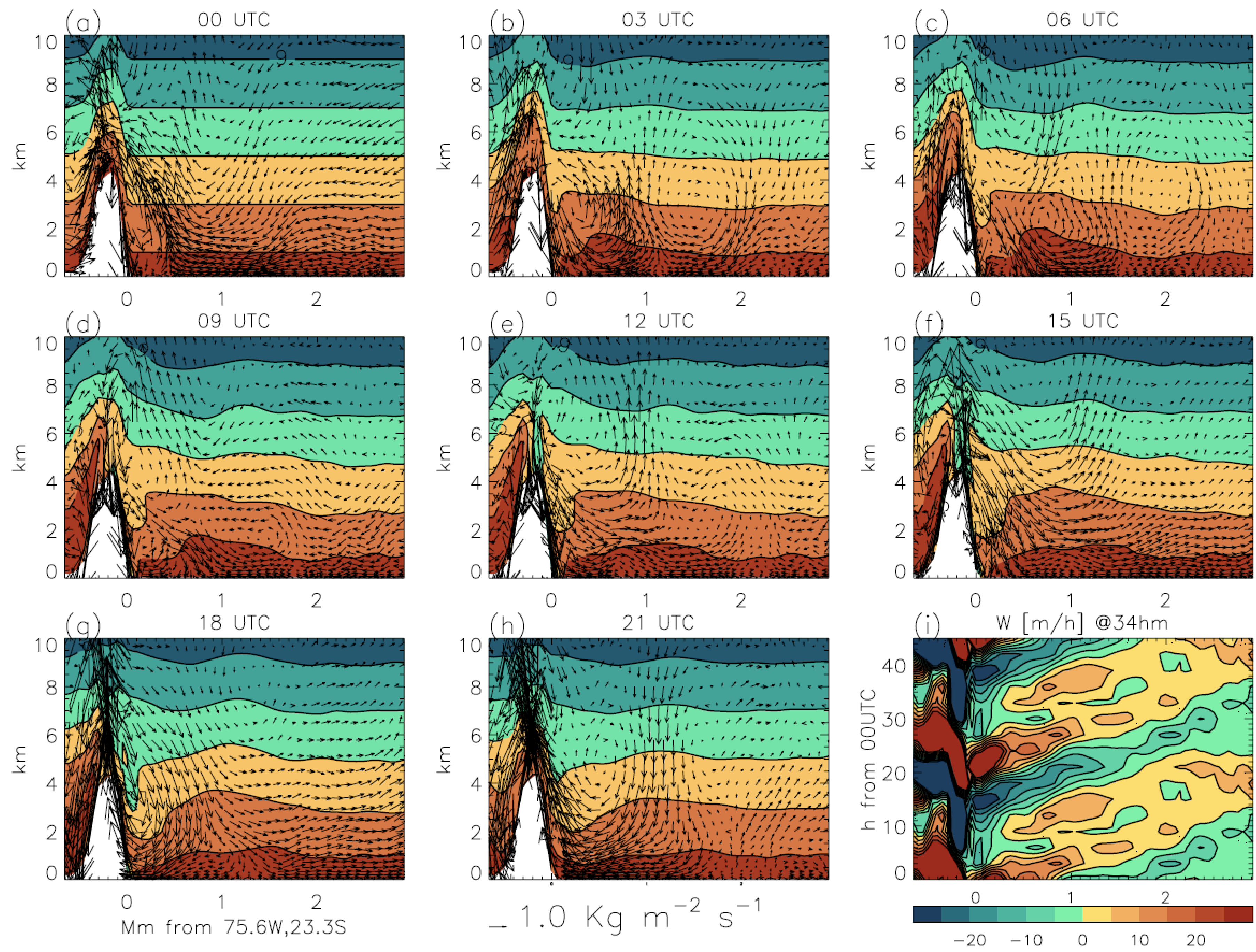

Fig. 6. (a–h) Snapshots of the mean circulation through a daily cycle along a great circle at a right angle to the South-Peruvian orographic slope and intersecting the coastline at 75.6° W, 23.3° S. The long-term mean circulation has been removed and average anomalies for the time of the day are shown as indicated at the top of each panel in hours UTC. The abscissae indicate offshore distances in Mm, and the ordinates vertical heights in km. The arrows represent two components of the flow, the offshore and the vertical mass fluxes (scale arrow at the bottom of panel **h**). The colour-filled contour lines depict the nominal displacement (exaggerated 10-fold) of constant-height surfaces at 00 UTC (panel **a**, shown at intervals of 2 km starting from 1 km) as obtained from the time-integrated anomalies in the vertical velocity. **(i)** Hovmueller diagram for the vertical velocity anomalies, in metres per hour, as a function of time (increasing upwards) and offshore distance for a twice repeated daily cycle.

III. weather systems in the EBUS

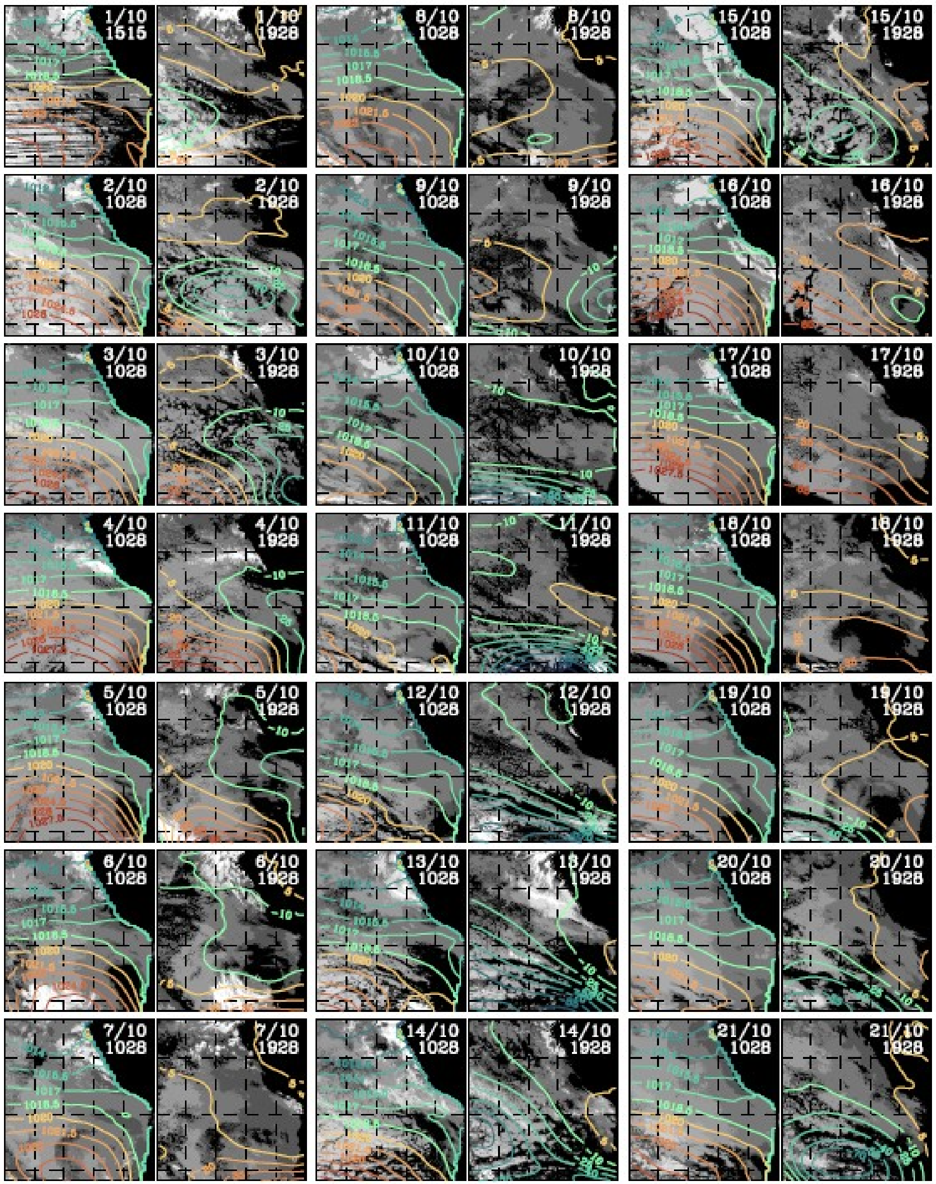

Fig. 14a. Twice-daily snapshots (UTC time as indicated) of the temperature difference ΔT between the OSTIA SSTs and the GOES Channel 5 brightness temperature. The gray colours indicate the presence of low clouds, with lighter shades indicative of higher clouds in deeper boundary layers. The contour interval for the shading is 3 K. Values of ΔT below 6 K are shown in black, and values above 35 K are shown in white (cf. Fig.14c). See text for full details. The contour lines in the night-time panels show the sea-level pressure for the previous 00:00 UTC. The contour interval is 1.5 hPa; the 1020 hPa line is drawn in light orange colour, and the 1018.5 hPa line in light cyan. On the day-time panels, contours of the zonally asymmetric part of the 500 hPa geopotential height field are drawn, for the subsequent 00:00 UTC. A contour interval of 15 m is used, with positive values (at and above 5 m) in orange/red, and negative values (at and below −10 m) in cyan/blue.

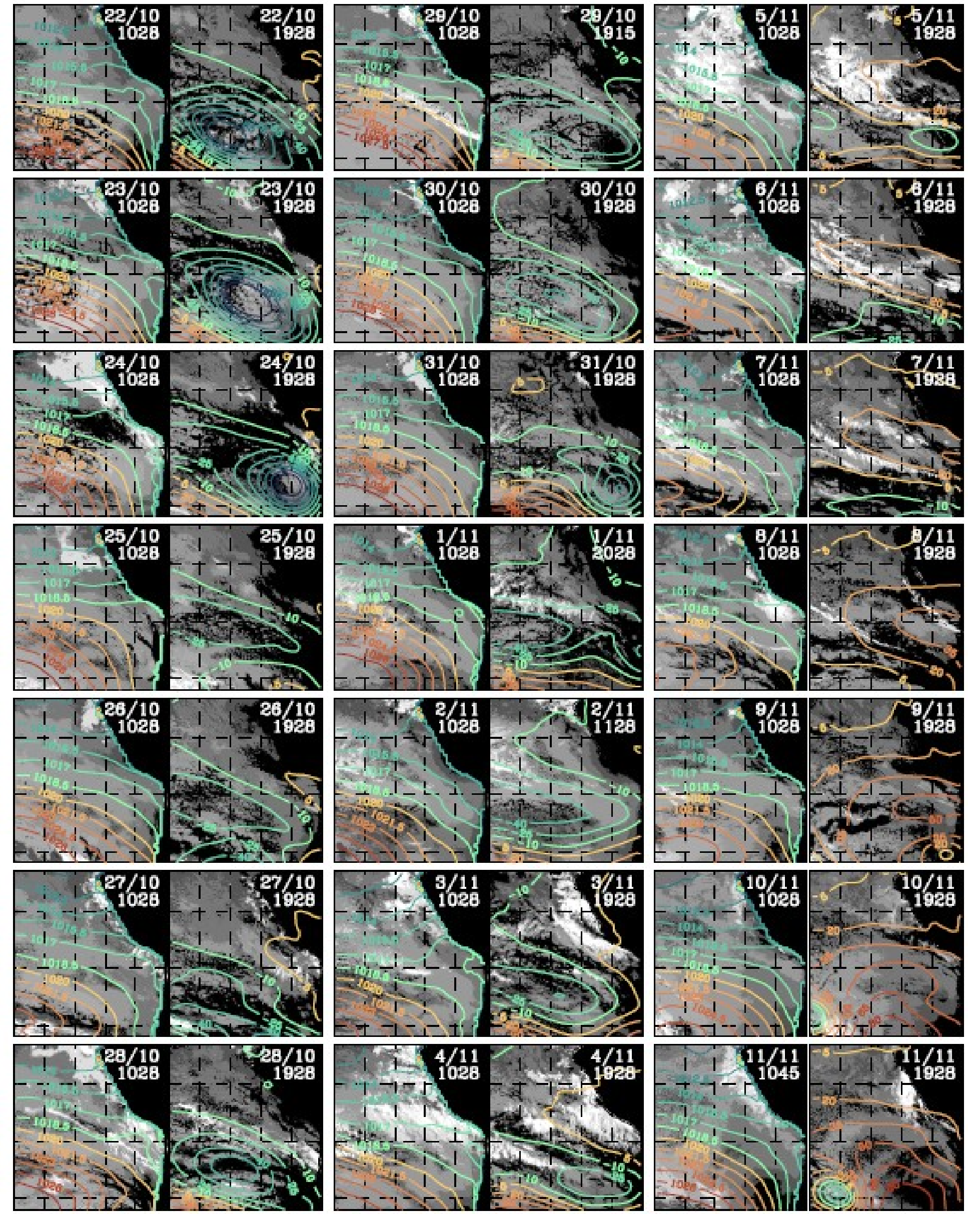

Fig. 14b. Continued.

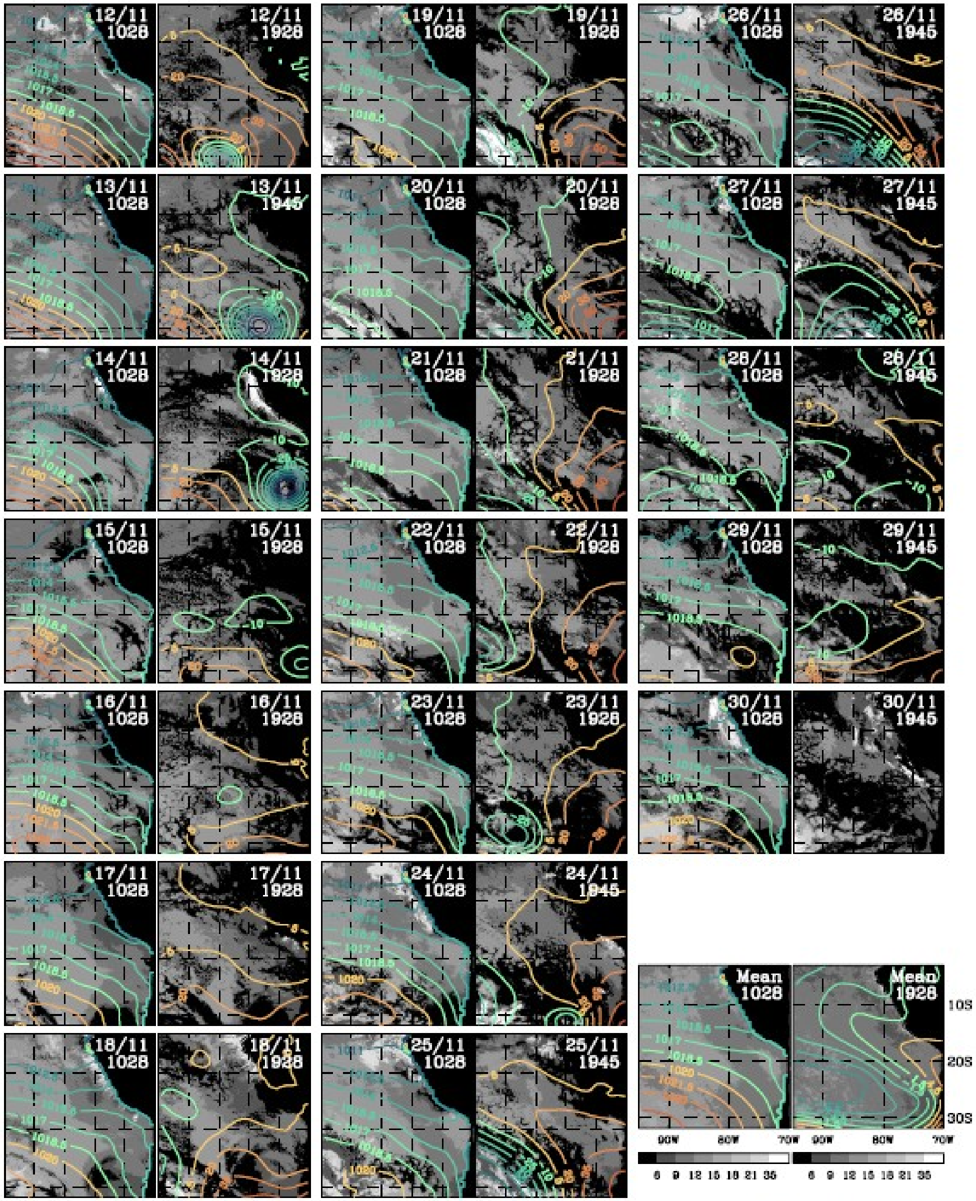

Fig. 14c. The final two panels show the October–November mean values of ΔT when cloud is present (determined as being when $3 < \Delta T < 35$ K) for the morning and afternoon times, with contours of mean pressure (overlaid on morning) and 500 hPa geopotential height (afternoon).

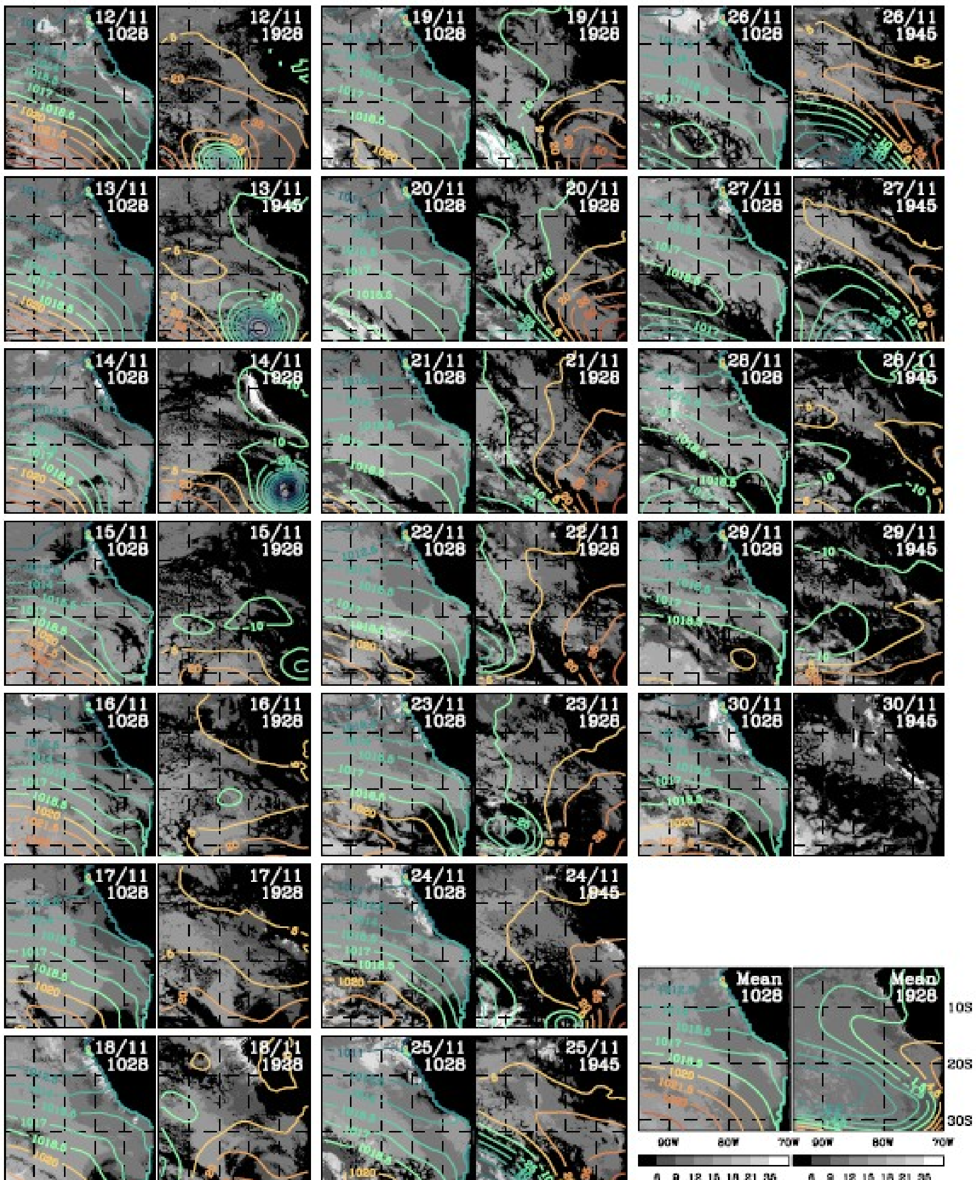

Fig. 14c. The final two panels show the October–November mean values of ΔT when cloud is present (determined as being when $3 < \Delta T < 35$ K) for the morning and afternoon times, with contours of mean pressure (overlaid on morning) and 500 hPa geopotential height (afternoon).

Main synoptic-scale disturbances affecting the Benguela coast

Coastally trapped lows (warm seasons)

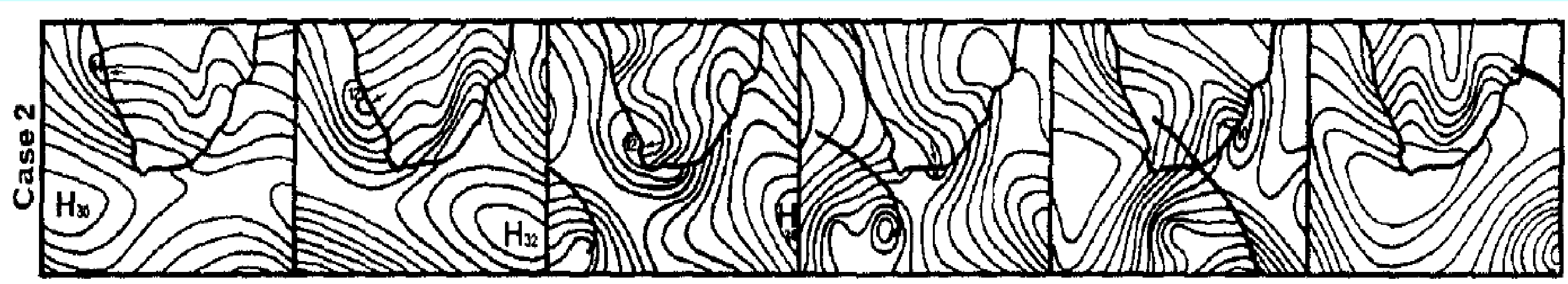

Reason 1996

Tropical-temperate troughs (DJF)

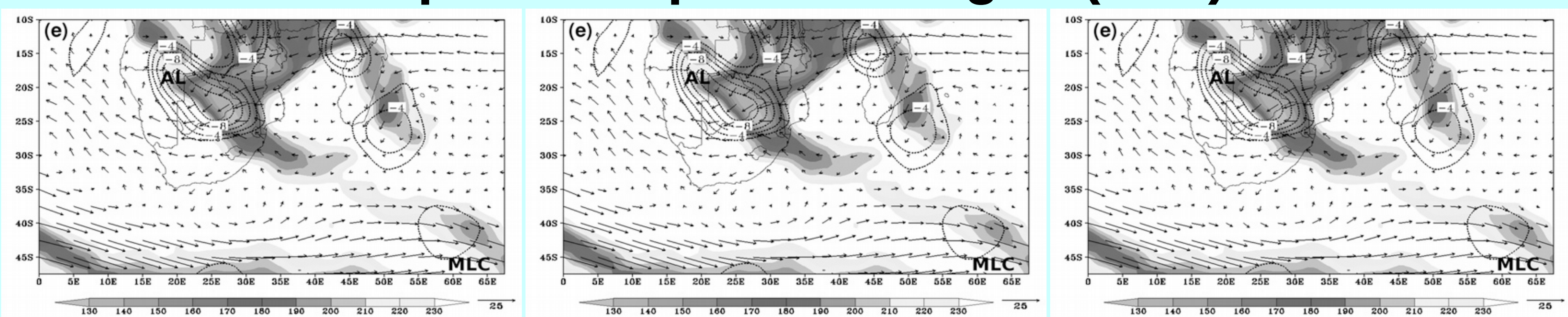

Hart et al. 2010

Cut-off lows

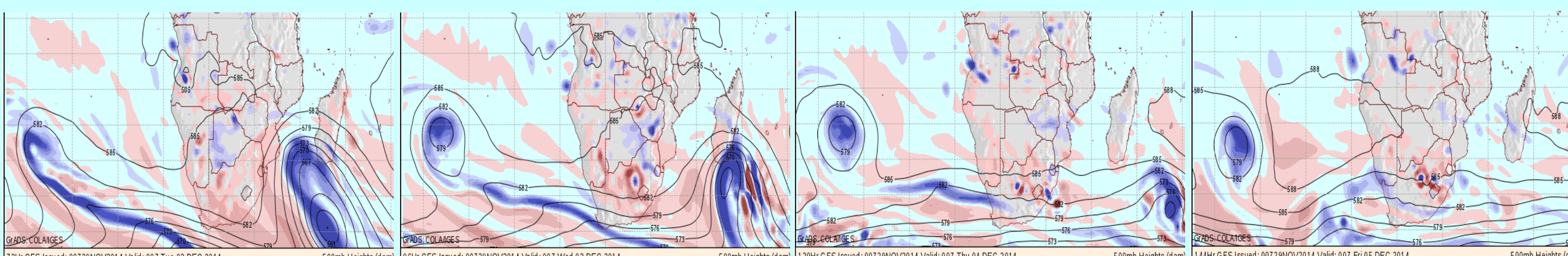

A few days ago

The link between mid-latitudes Rossby waves and surface weather

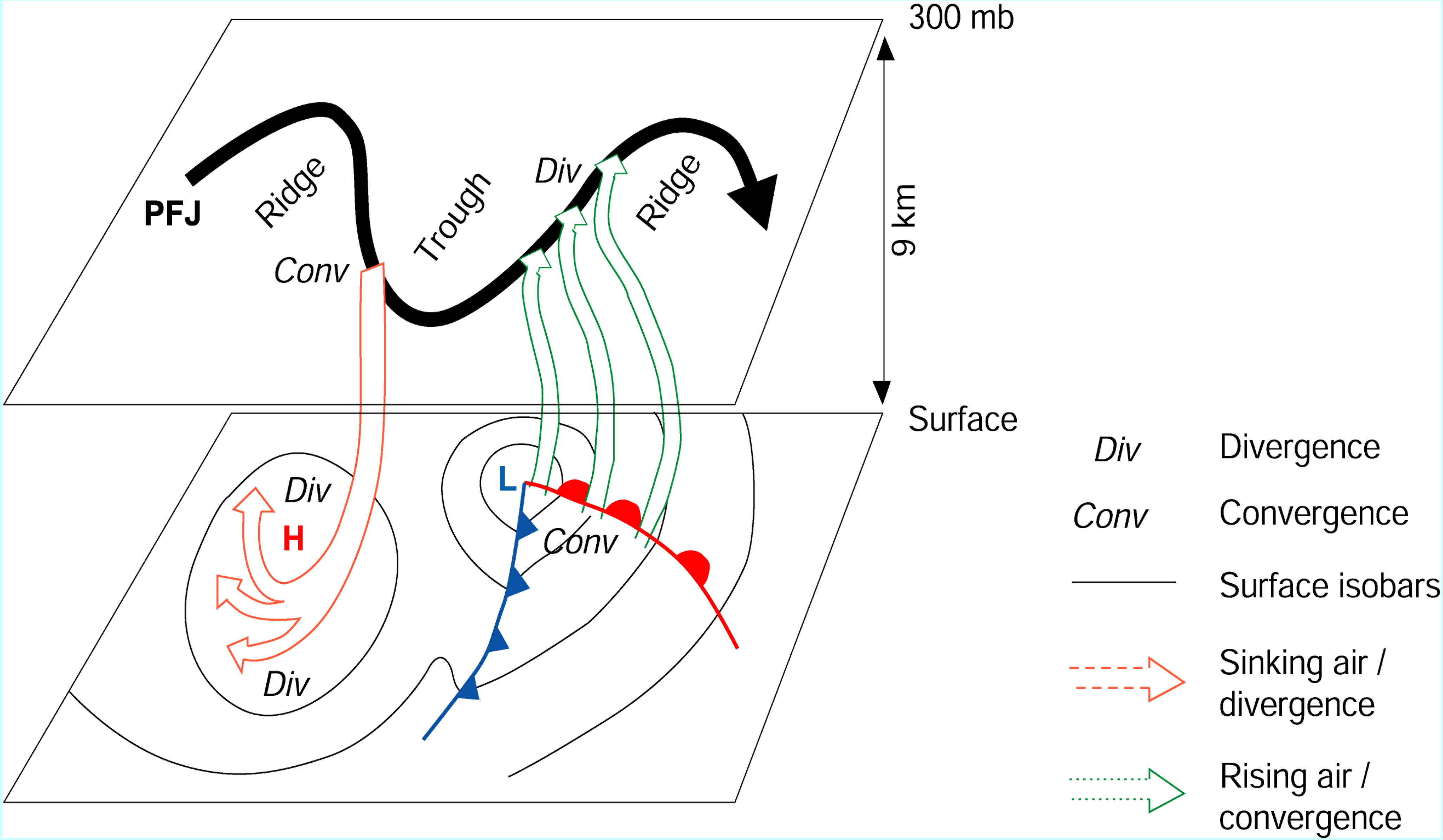

TTTs

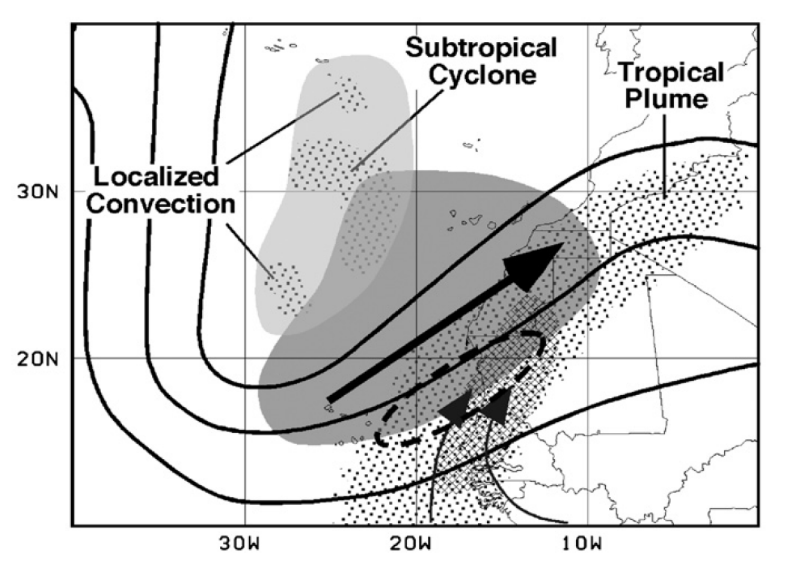

Knippertz 2006

- Breaking LC1 cyclone wave(train) with low-latitude PV streamer provides low-level vorticity and dynamic uplift

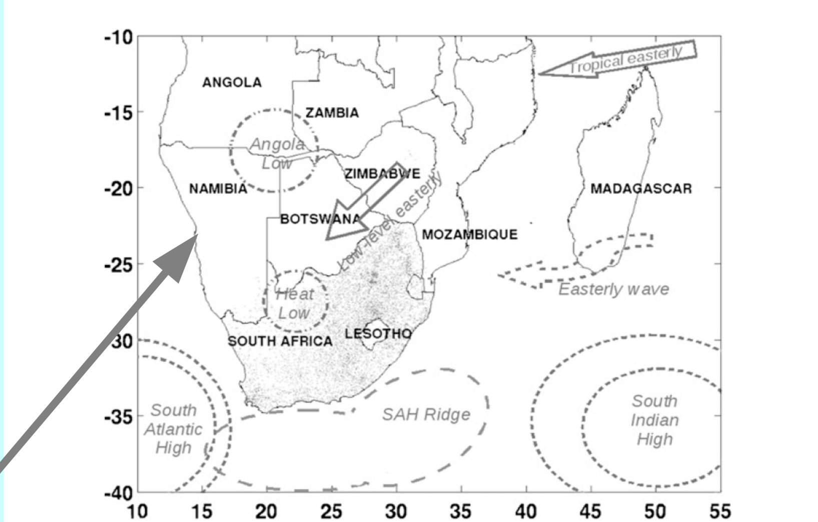

Hart et al. 2002

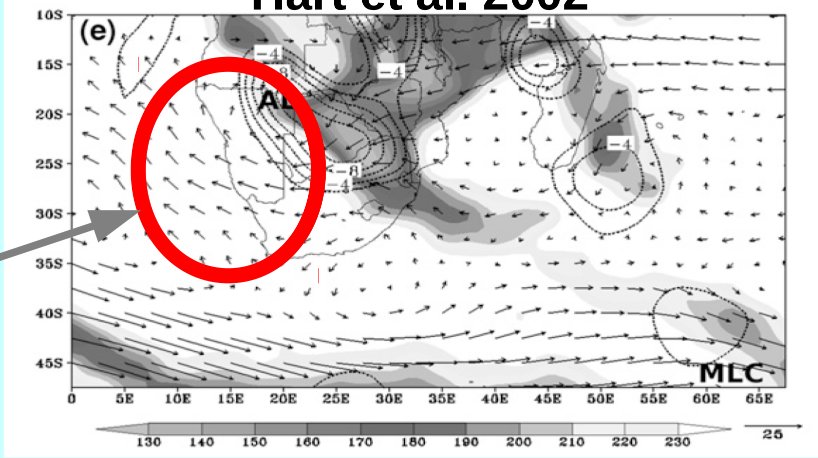

- Couples with tropical low-level winds providing moisture & triggering convection
- Over southern Africa, important role of the Angola Low
- Can cause intense both on- and off-short wind anomalies of the duration of a few days

Mid-tropospheric cut-off lows: genesis

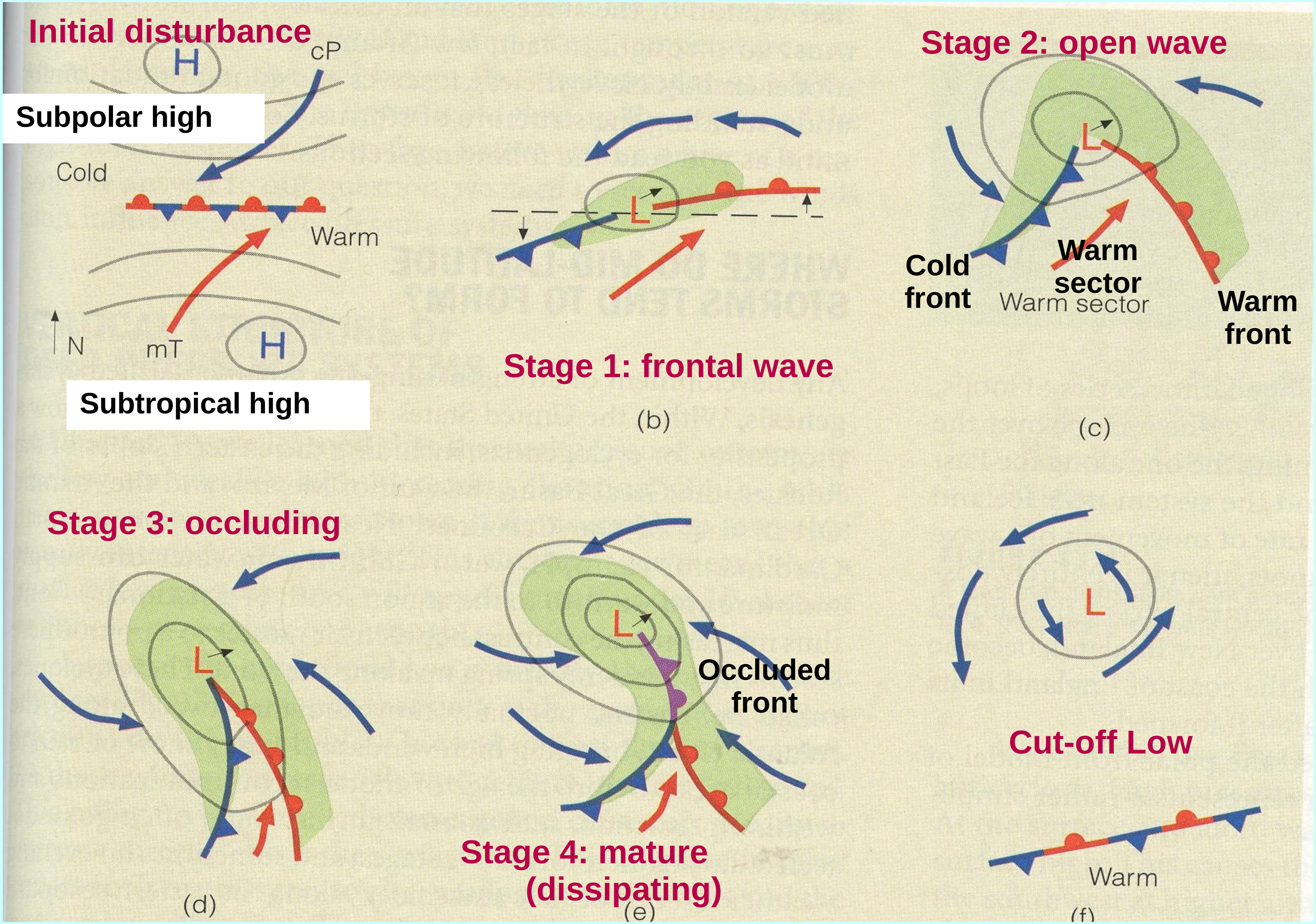

CLs

- Brief (1-4 days) but ubiquitous
- Synoptic forcing provided by large-scale mid-latitude ridging
- Generates down-slope flow into the LLJ area
- Warm advection etc
- Shallow system
- Moves along inversion as coastal Ke wave, with typical speed of ~20 m/s (Reason 1996)
- Can go round all of Southern Africa (Gill 1982)

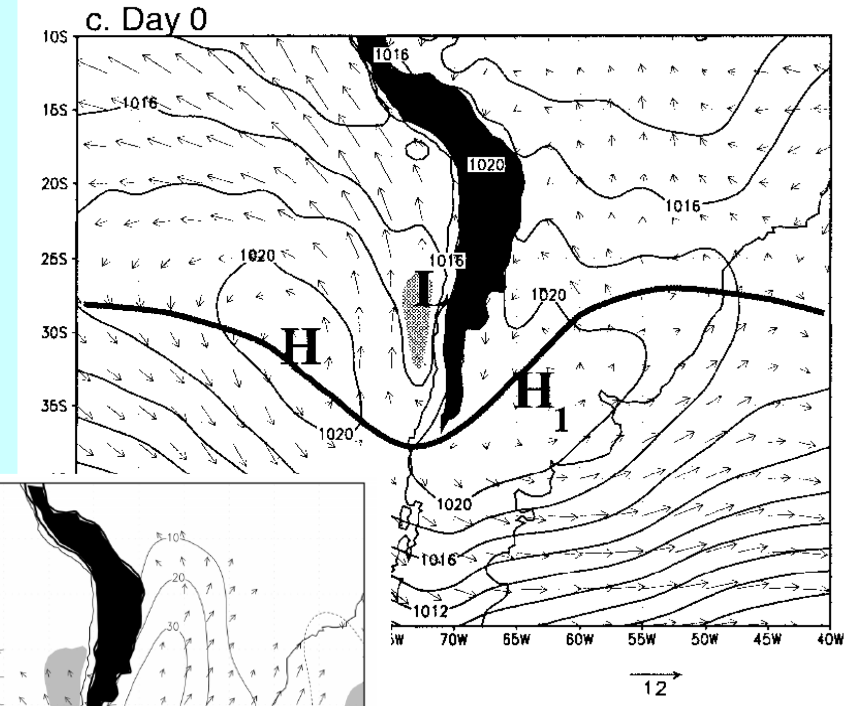

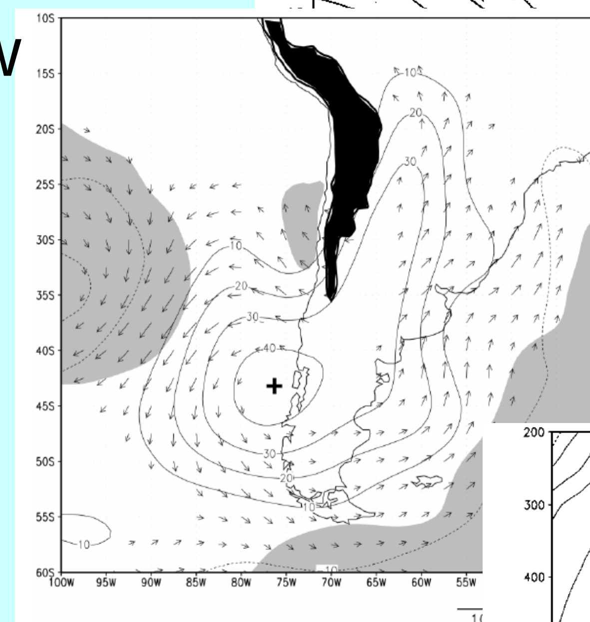

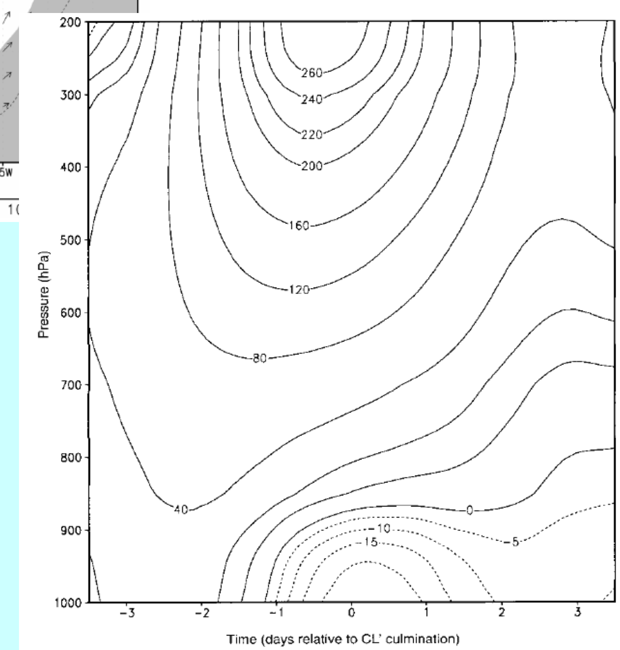

Garreaud et al. 2002

Coastal Lows along the Subtropical West Coast of South America: Mean Structure and Evolution

René D. Garreaud, José A. Rutllant, and Humberto Fuenzalida

Department of Geophysics, Universidad de Chile, Santiago, Chile

(Manuscript received 22 November 2000, in final form 7 June 2001)

These so-called coastal lows (CLs) occur up to five times per month in all seasons, although they are better defined from fall to spring.

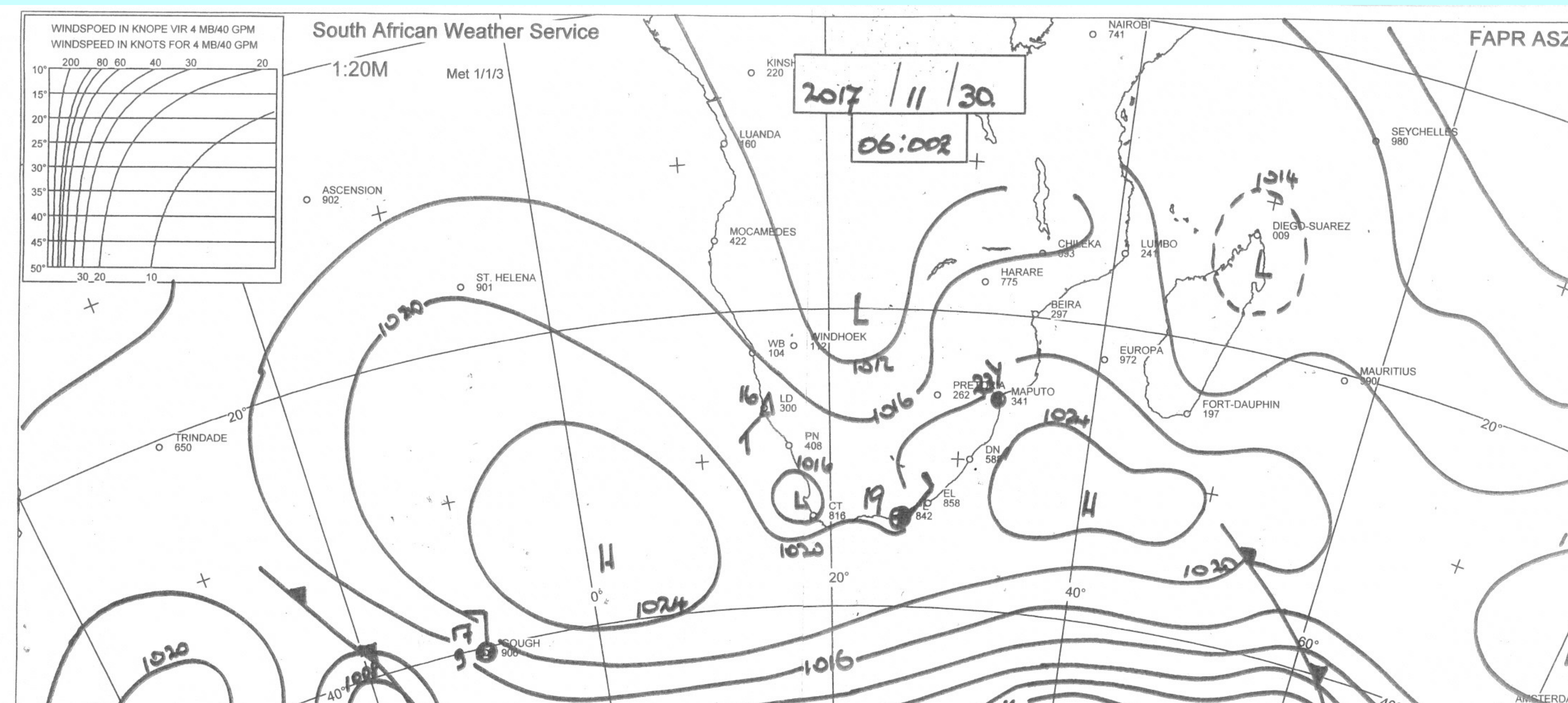

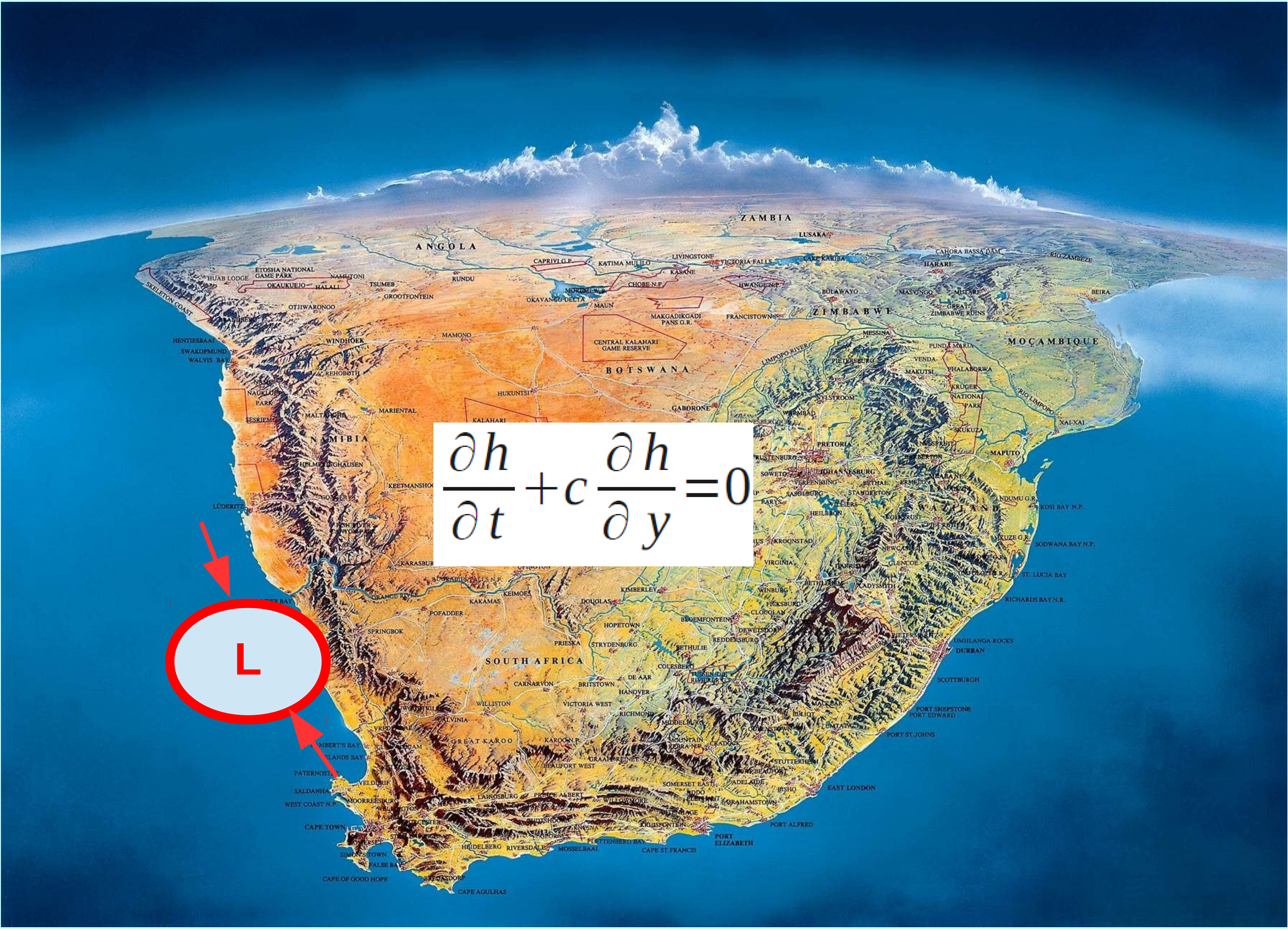

$$\frac{\partial h}{\partial t}+c\frac{\partial h}{\partial y}=0$$

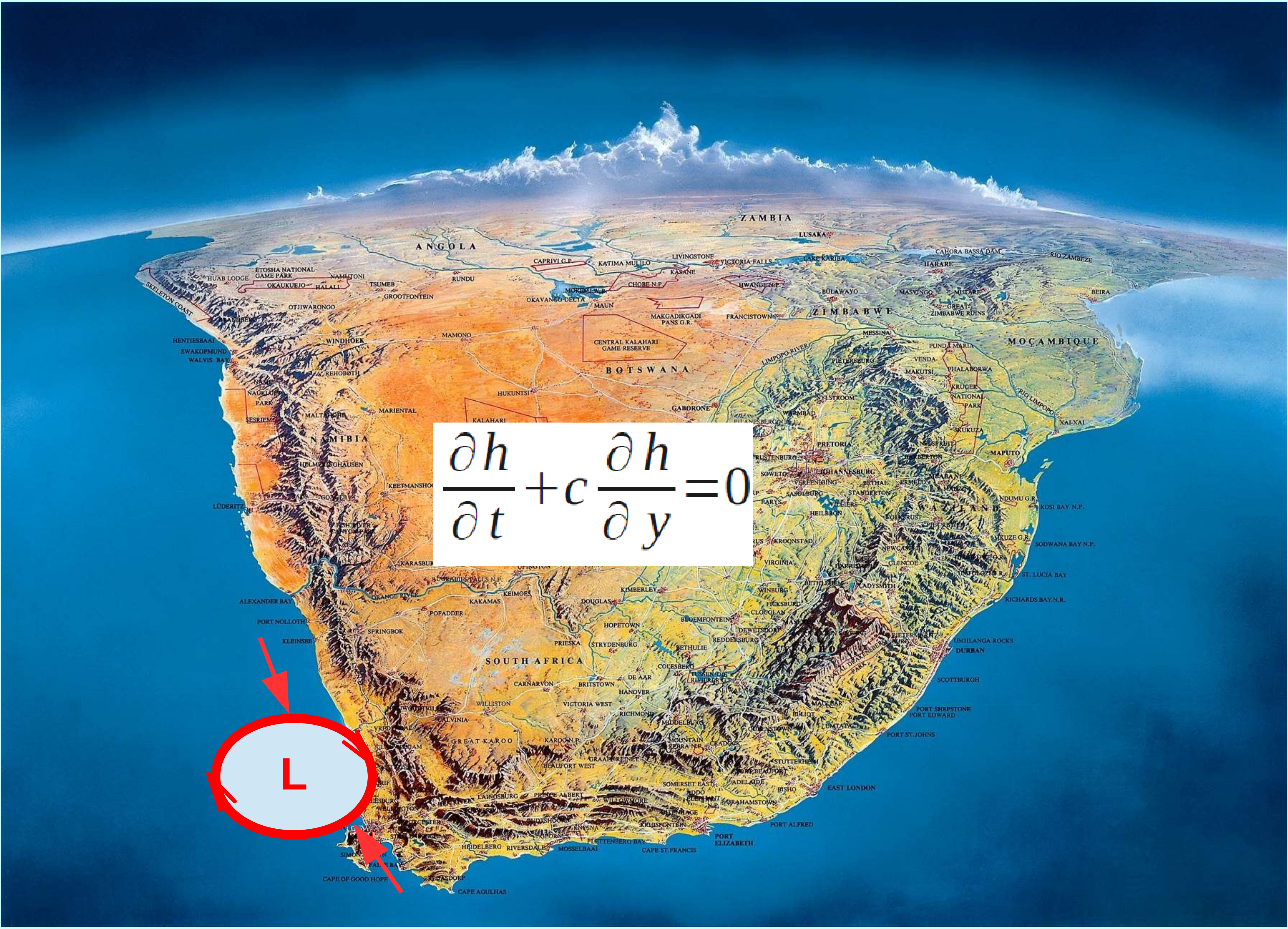

$$\frac{\partial h}{\partial t} + c\,\frac{\partial h}{\partial y} = 0$$

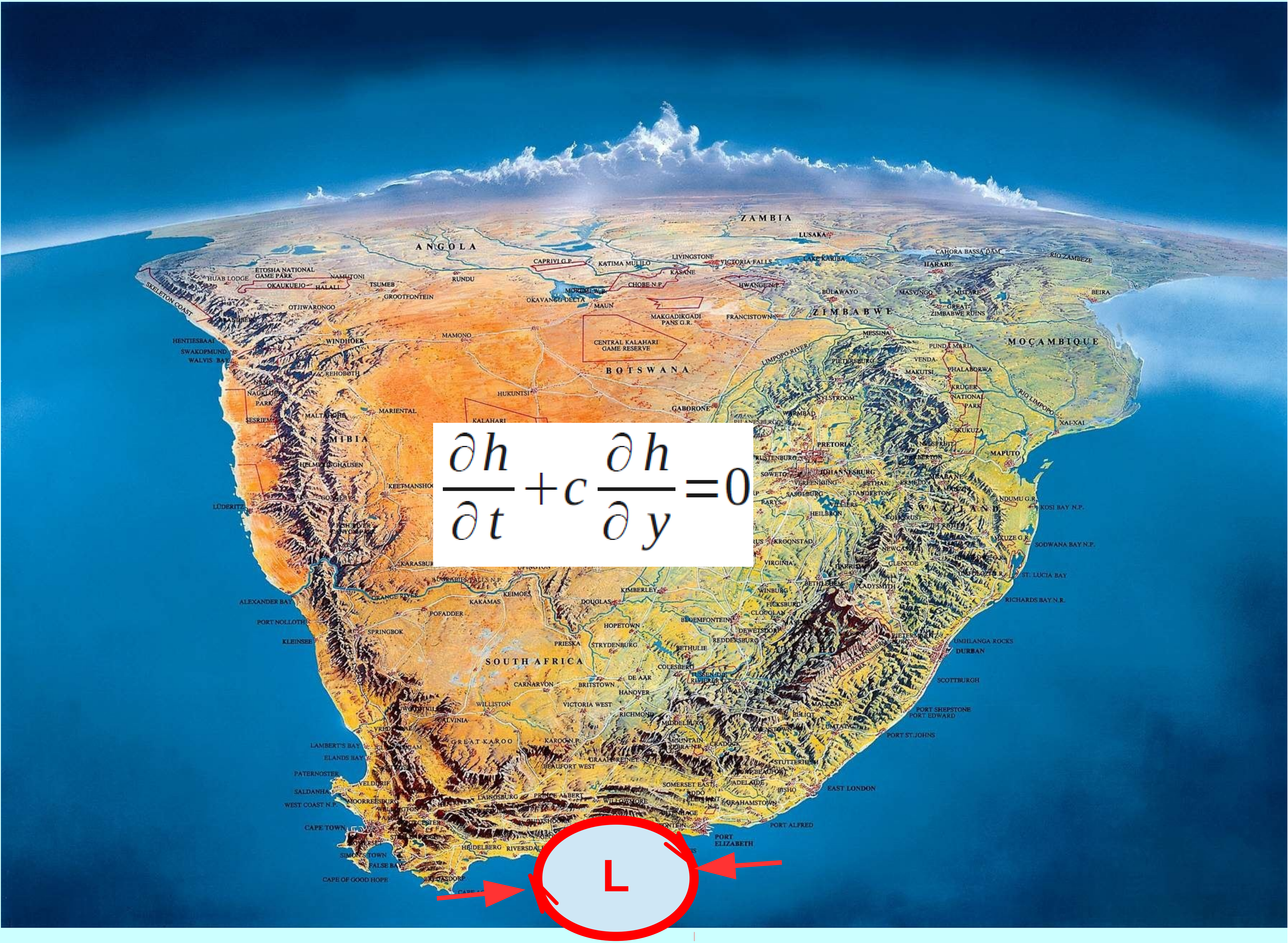

$$\frac{\partial h}{\partial t}+c\frac{\partial h}{\partial y}=0$$


30.11.2017 12:48


01.12.2017

Synoptic-scale frontal forcing can dominate short time scales

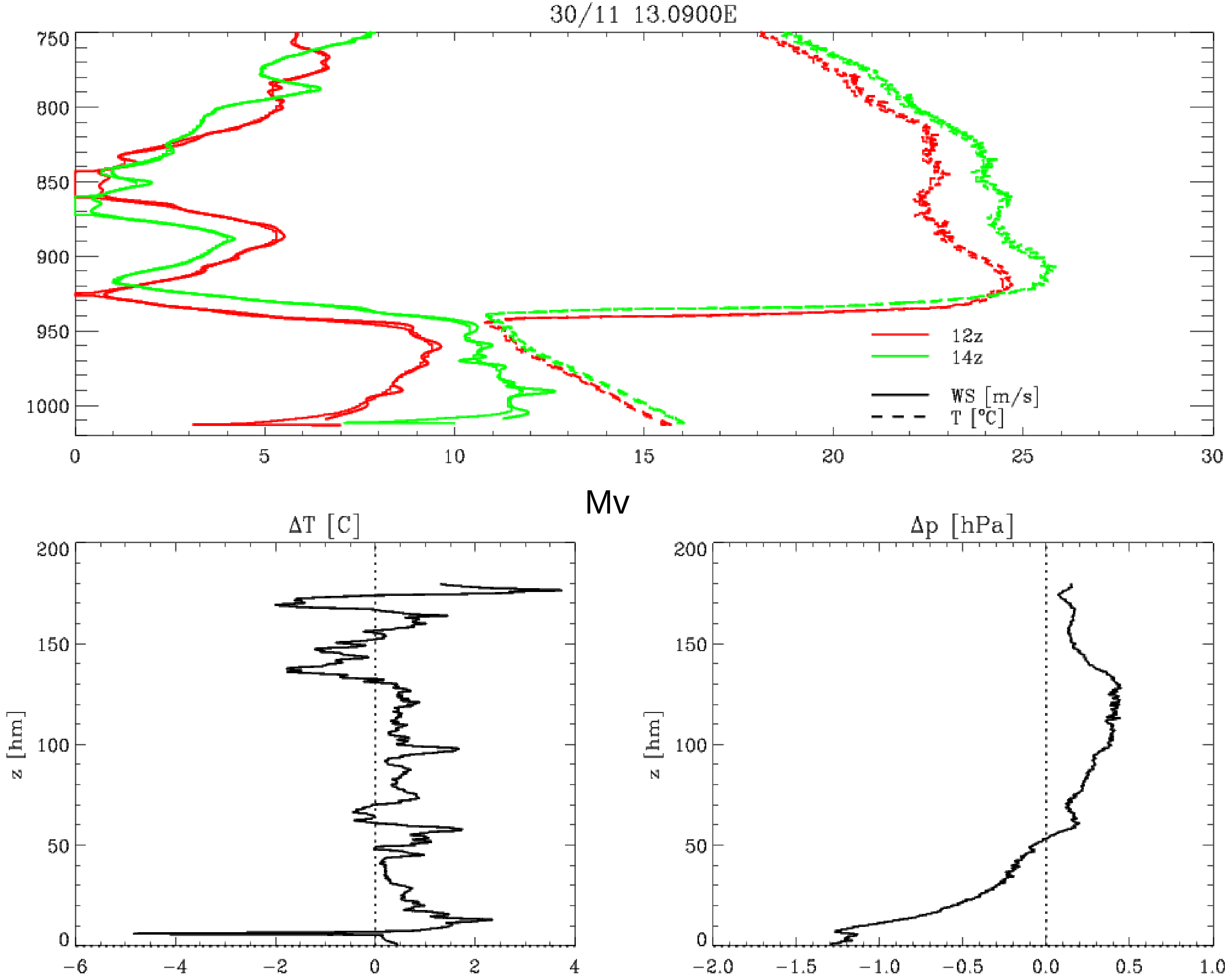


30.11.2017 14:28


30.11.2017 14:57

Init: Thu,30NOV2017 12Z 500 hPa Geopot. (gpdm), T (C), Bodendruck (hPa)

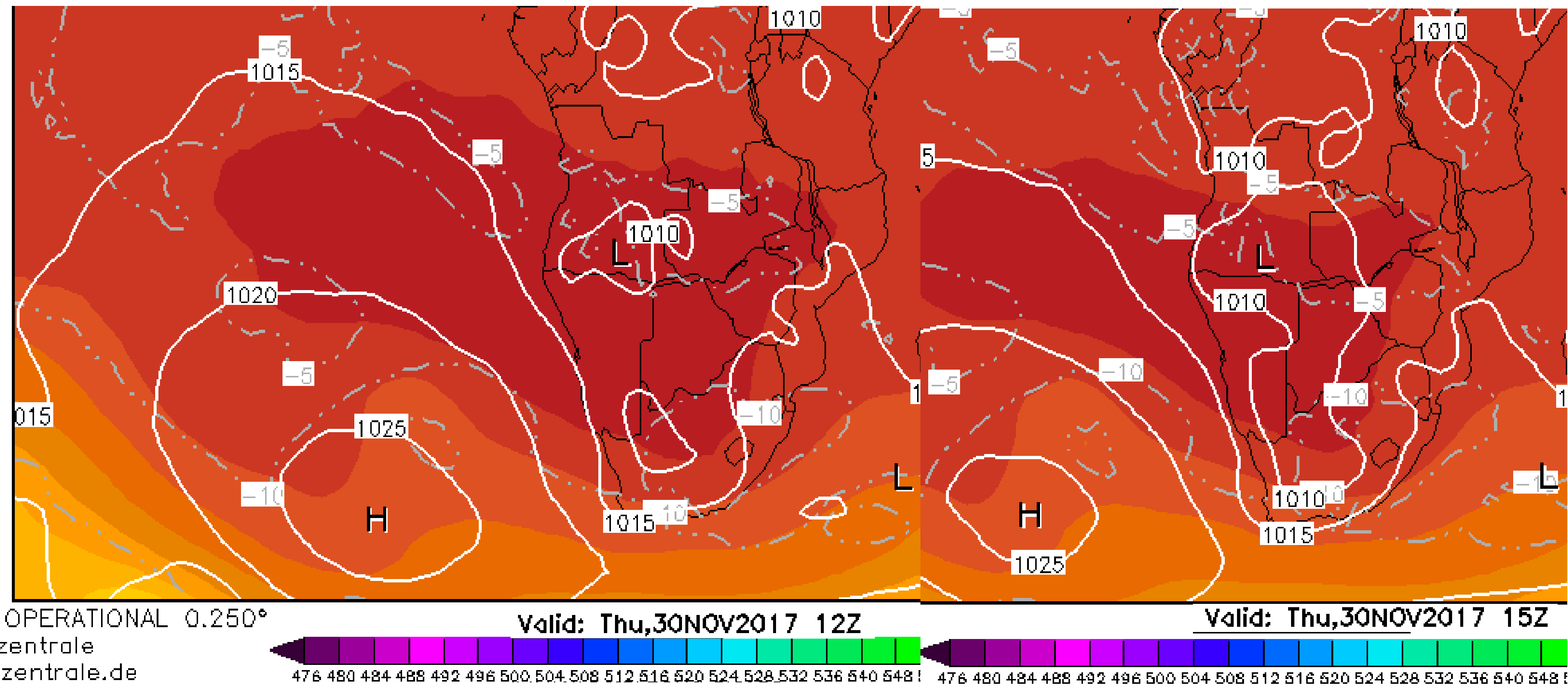

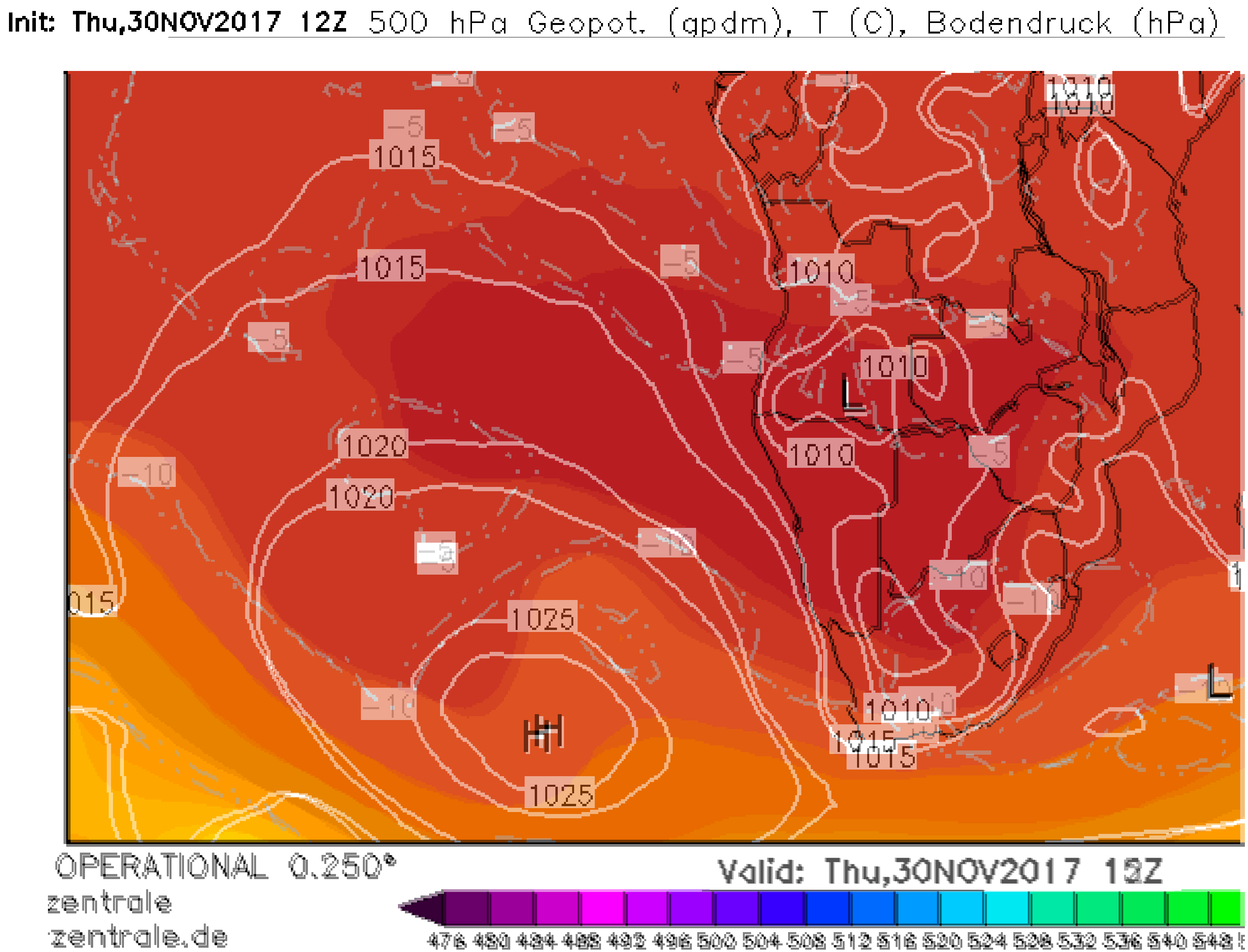
Init: Thu,30NOV2017 12Z 500 hPa Geopot. (gpdm), T (C), Bodendruck (hPa)
OPERATIONAL 0.250°
zentrale
zentrale.de
Valid: Thu,30NOV2017 12Z
476 480 484 488 492 496 500 504 508 512 516 520 524 528 532 536 540 544
1015
1020
1025
1010
-5
-10
H
L

IV. atmospheric observations and models in the EBUS

IV. atmospheric observations and models in the EBUS

Radiosonde profiles against reanalysis products in the Benguela

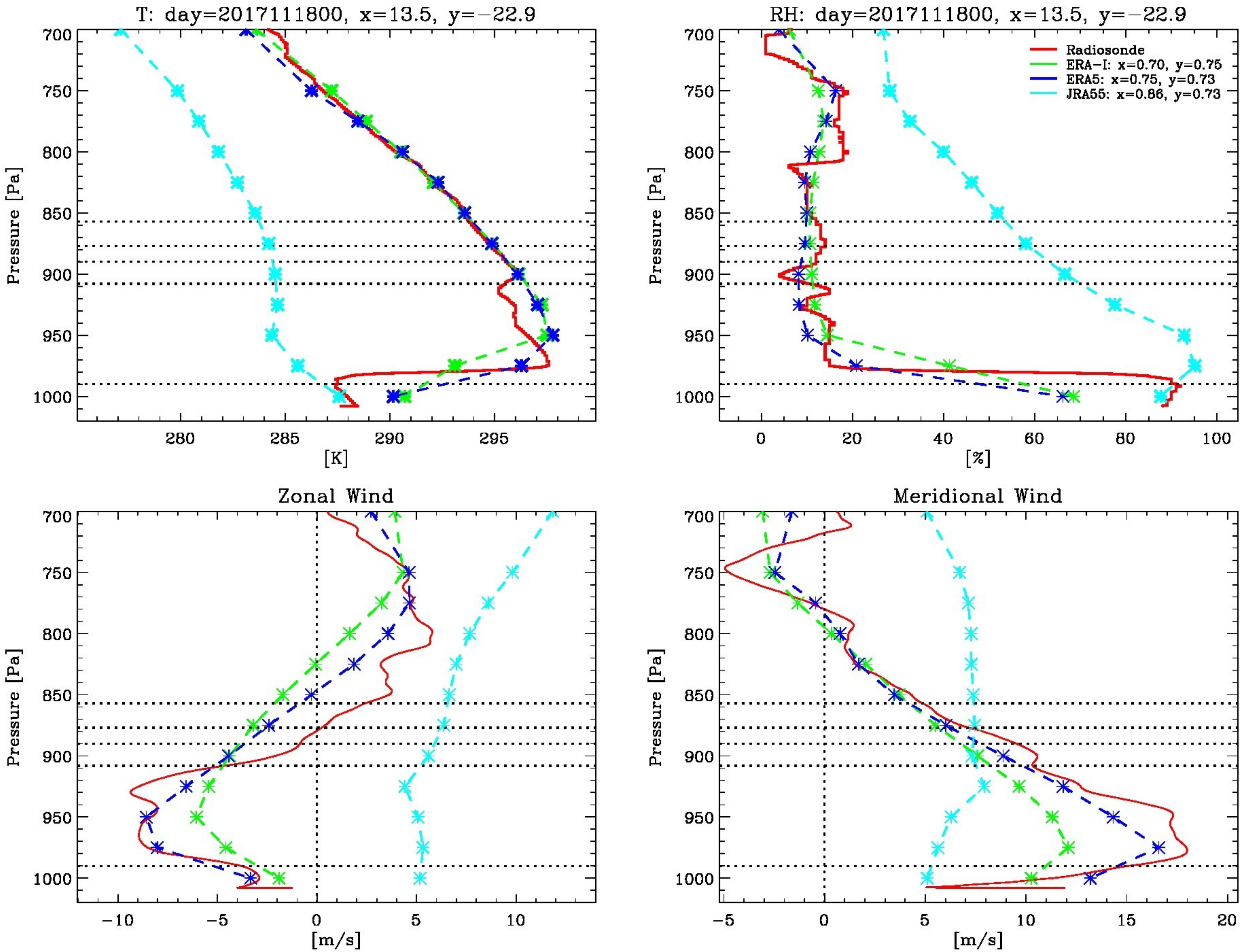

Radiosonde profiles against reanalysis products in the Benguela

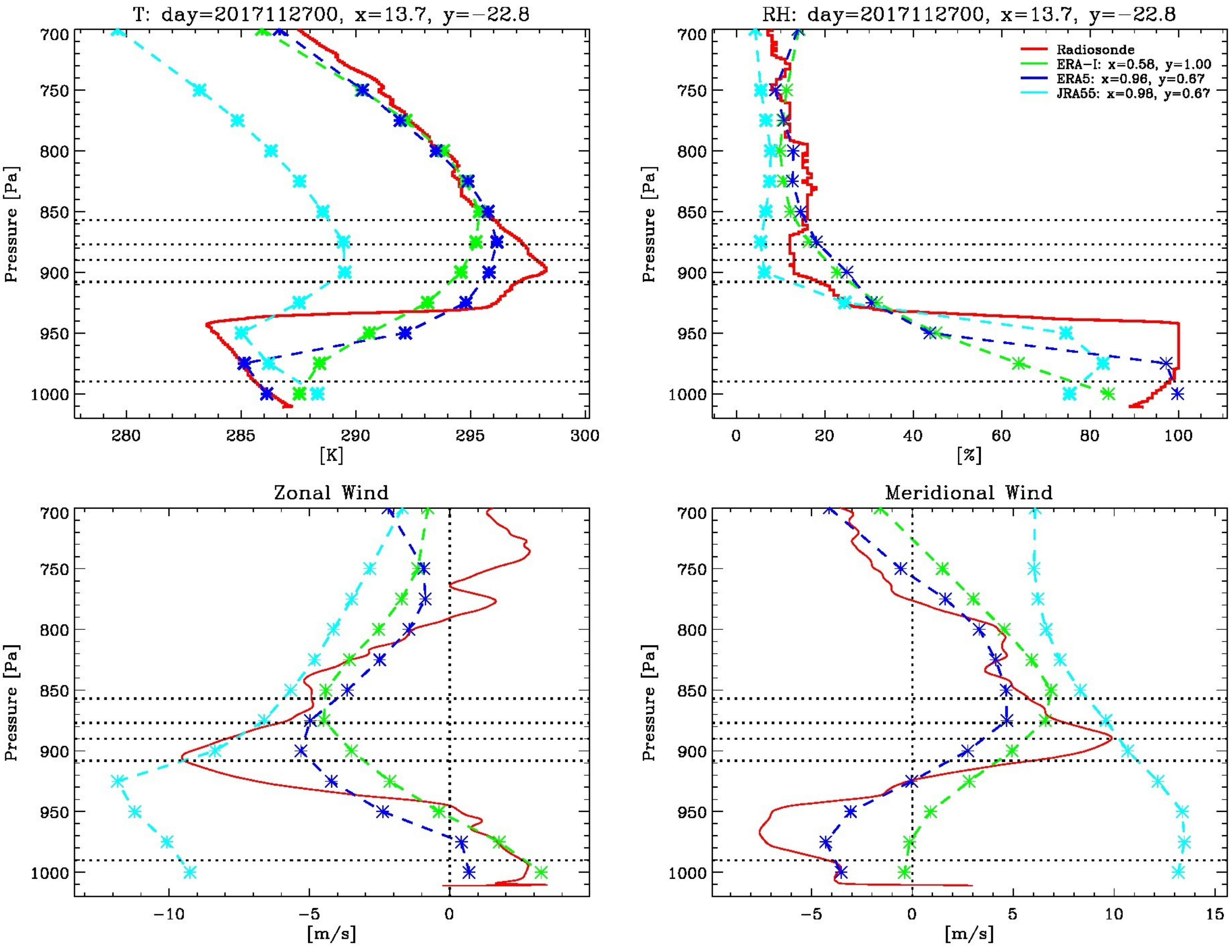

The scarcity of in-situ data acquisition in operation product leads to systematic biases in the reanalyses which tend to reflect common model biases.

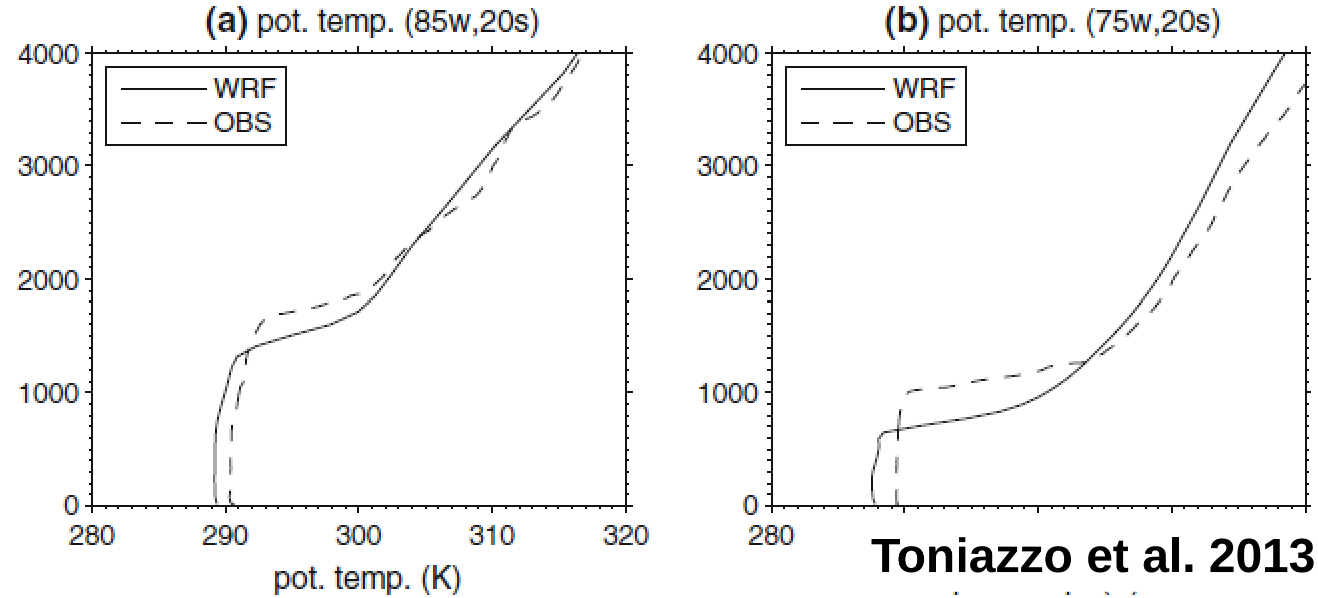

Toniazzo et al. 2013

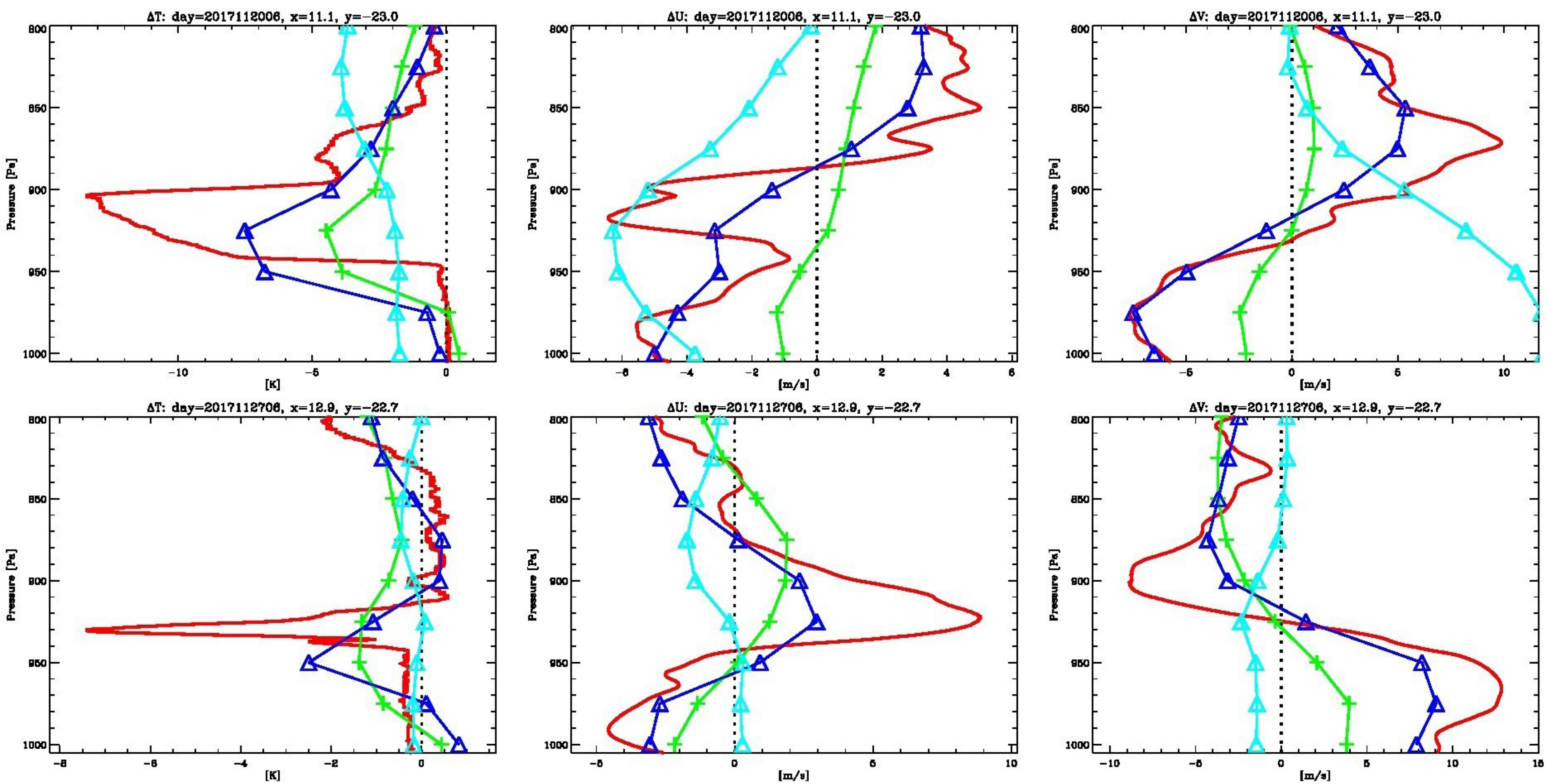

by

Kathleen Rhona Peard

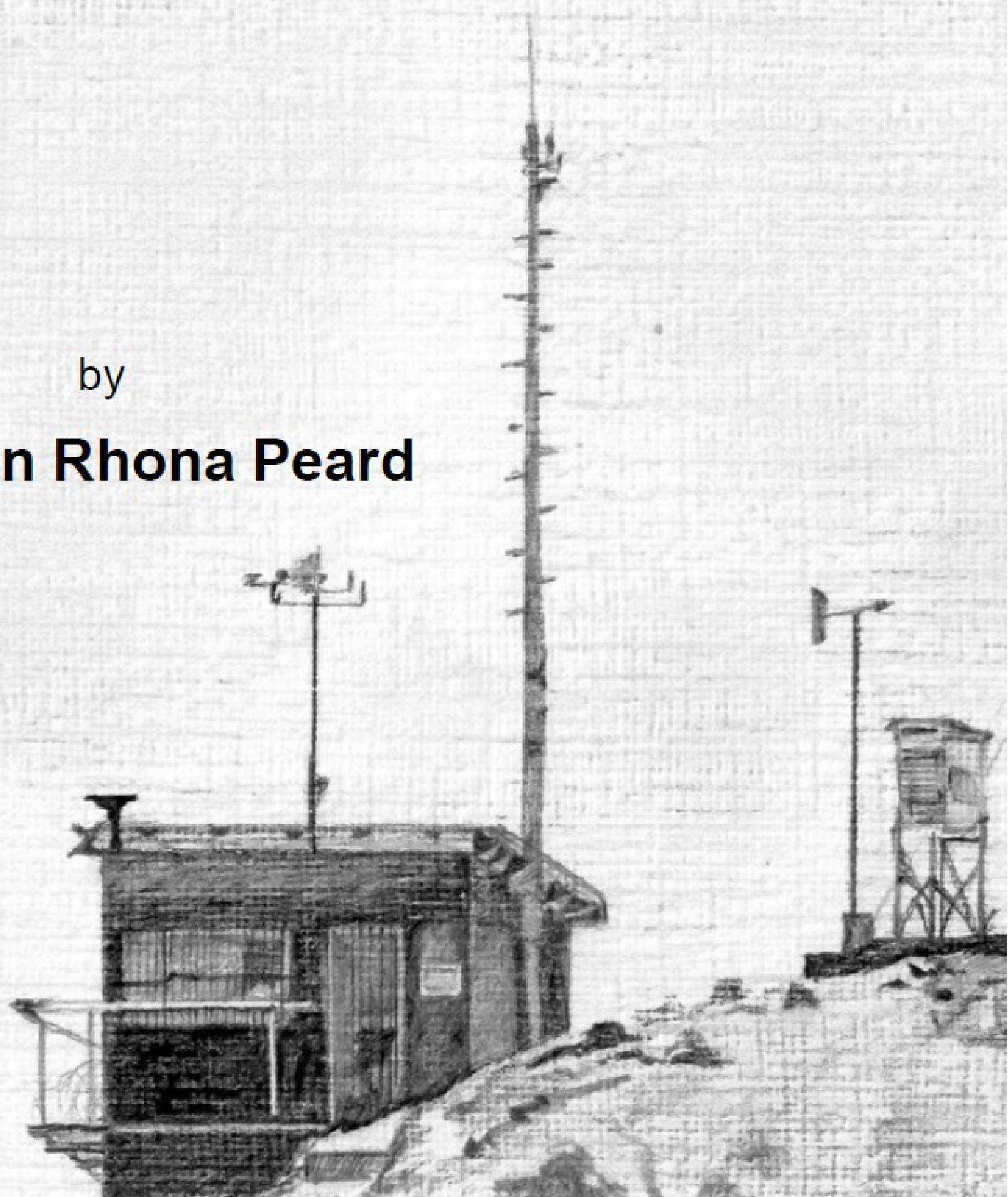

Thesis Presented for the Degree of

MASTER OF SCIENCE

In the Department of Oceanography

UNIVERSITY OF CAPE TOWN

May 2007

Acquired in-situ wind observations (Cape Diaz, Luedritz)

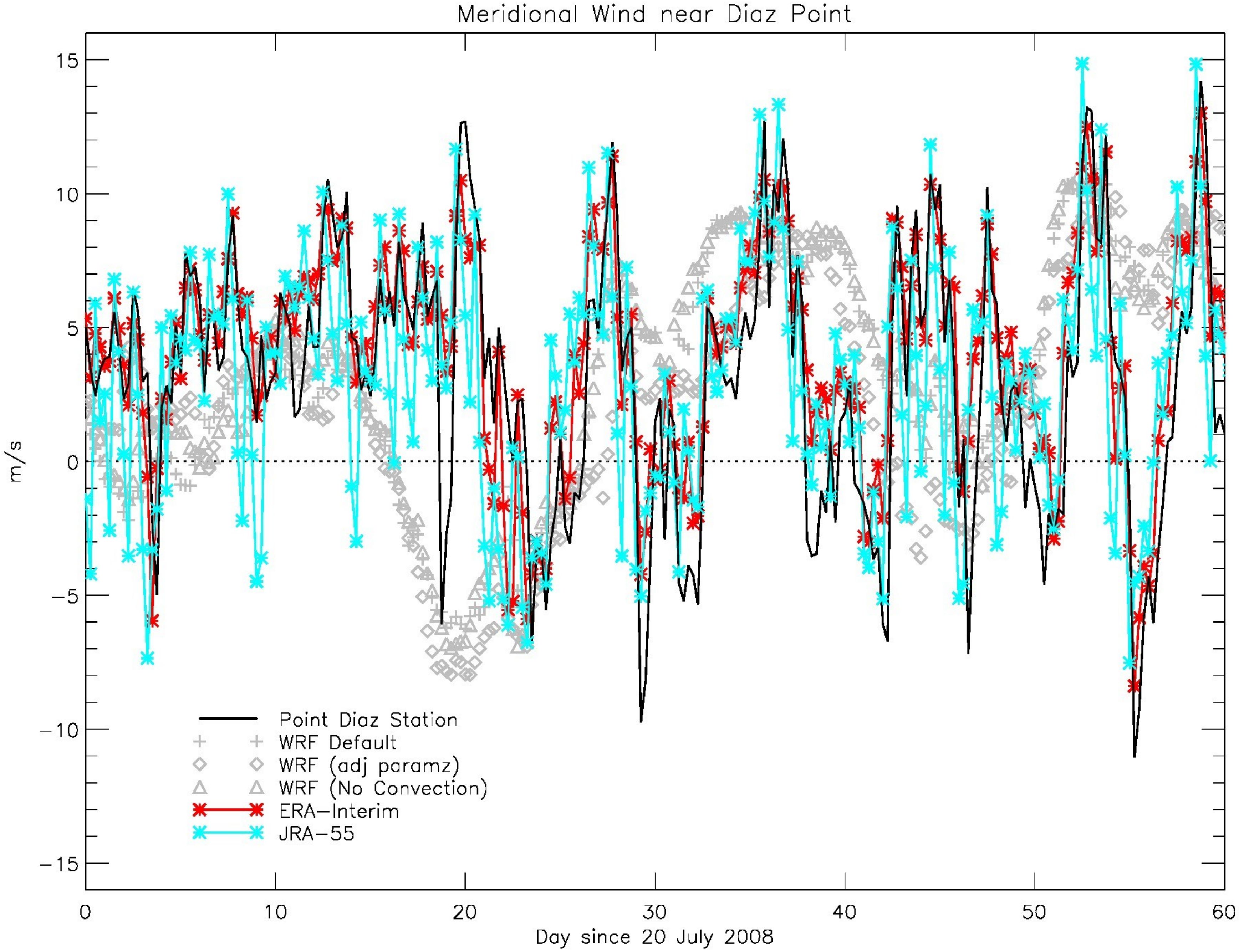

Courtesy: Jean-Paul Roux

A recent *intercomparison* of reanalysis and satellite products

Contents lists available at ScienceDirect

Ocean Modelling

journal homepage: www.elsevier.com/locate/ocemod

Surface winds from atmospheric reanalysis lead to contrasting oceanic forcing and coastal upwelling patterns

Fernando G. Taboada[*,a,b], Charles A. Stock[a], Stephen M. Griffies[a], John Dunne[a], Jasmin G. John[a], R. Justin Small[c], Hiroyuki Tsujino[d]

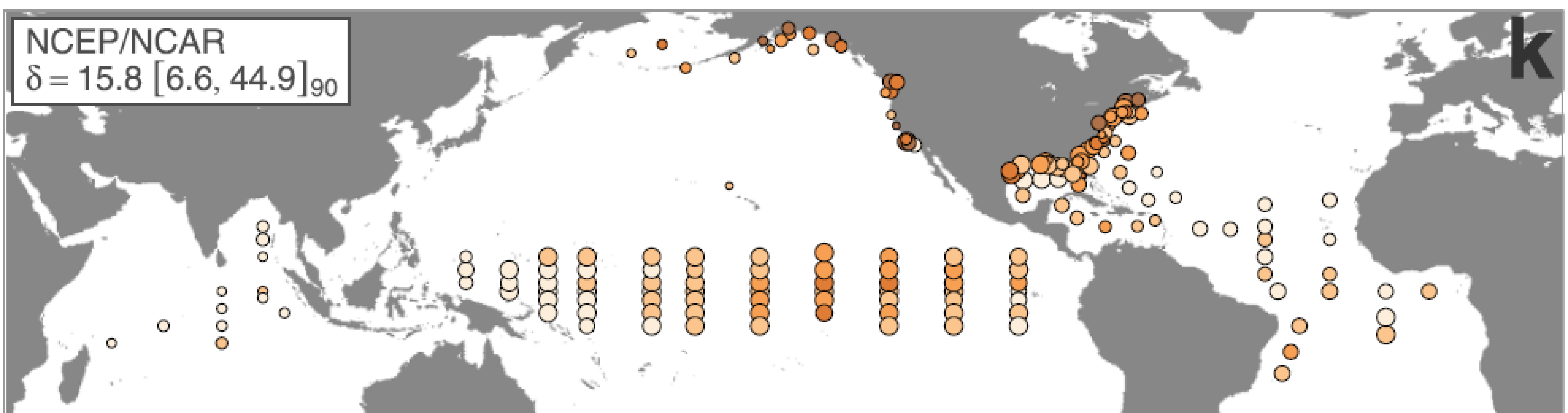

A few important points

I. *In contrasts with the large-scale trade winds, the surface winds of the EBUS undergo significant high-frequency variability*

   i. *Inertial (diurnal cycle)*

   ii. *Mesoscale (coastal lows)*

   iii. *Synoptic (TTTs and mid-latitude ridges/troughs)*

II. **This variability is controlled by changes in temperatures in the free troposphere, mainly via vertical advection**

III. **In-situ observations are (increasingly) scarce in some EBUS (e.g. Benguela)**

IV. **Reliance on model-generated data can lead to misestimations of the “true” atmospheric state in these areas.**